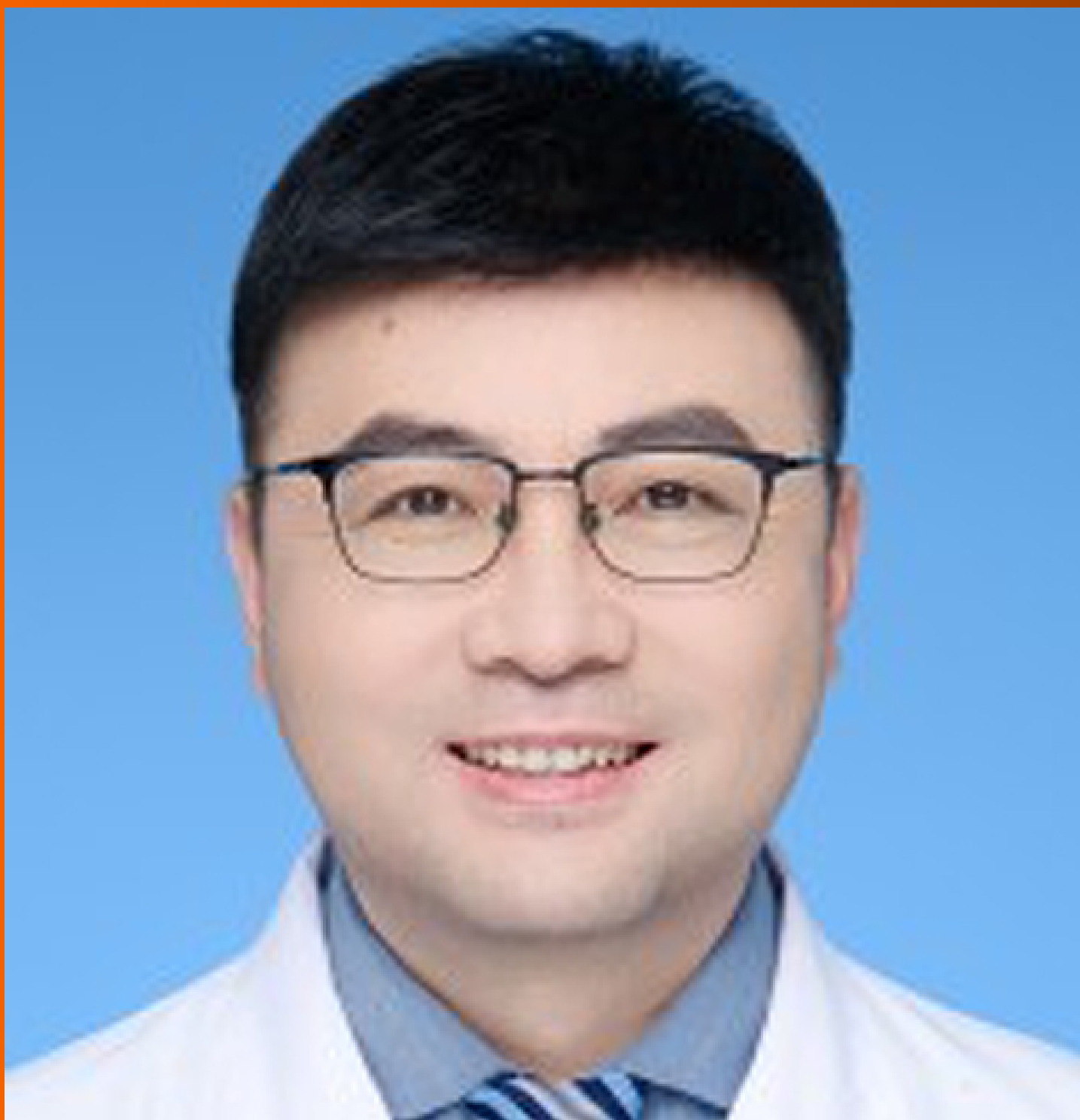


# World Journal of *Gastrointestinal Oncology*

*World J Gastrointest Oncol* 2024 April 15; 16(4): 1091-1675



**EDITORIAL**

- 1091 Parallel pathways: A chronicle of evolution in rectal and breast cancer surgery  
*Pesce A, Fabbri N, Iovino D, Feo CV*
- 1097 Hepatitis B virus genotypes in precision medicine of hepatitis B-related hepatocellular carcinoma: Where we are now  
*Sukowati CHC, Jayanti S, Turyadi T, Muljono DH, Tiribelli C*

**REVIEW**

- 1104 Novel milestones for early esophageal carcinoma: From bench to bed  
*Qi JH, Huang SL, Jin SZ*
- 1119 Colorectal cancer screening: A review of current knowledge and progress in research  
*Lopes SR, Martins C, Santos IC, Teixeira M, Gamito É, Alves AL*
- 1134 New avenues for the treatment of immunotherapy-resistant pancreatic cancer  
*Silva LGO, Lemos FFB, Luz MS, Rocha Pinheiro SL, Calmon MDS, Correa Santos GL, Rocha GR, de Melo FF*

**MINIREVIEWS**

- 1154 Present situation of minimally invasive surgical treatment for early gastric cancer  
*Li CY, Wang YF, Luo LK, Yang XJ*
- 1166 Mixed neuroendocrine non-neuroendocrine neoplasms in gastroenteropancreatic tract  
*Díaz-López S, Jiménez-Castro J, Robles-Barraza CE, Ayala-de Miguel C, Chaves-Conde M*
- 1180 Esophageal cancer screening, early detection and treatment: Current insights and future directions  
*Qu HT, Li Q, Hao L, Ni YJ, Luan WY, Yang Z, Chen XD, Zhang TT, Miao YD, Zhang F*

**ORIGINAL ARTICLE****Retrospective Cohort Study**

- 1192 Pre-operative enhanced magnetic resonance imaging combined with clinical features predict early recurrence of hepatocellular carcinoma after radical resection  
*Chen JP, Yang RH, Zhang TH, Liao LA, Guan YT, Dai HY*
- 1204 Clinical analysis of multiple primary gastrointestinal malignant tumors: A 10-year case review of a single-center  
*Zhu CL, Peng LZ*

**Retrospective Study**

- 1213** Predictive model for non-malignant portal vein thrombosis associated with cirrhosis based on inflammatory biomarkers  
*Nie GL, Yan J, Li Y, Zhang HL, Xie DN, Zhu XW, Li X*
- 1227** Predictive modeling for postoperative delirium in elderly patients with abdominal malignancies using synthetic minority oversampling technique  
*Hu WJ, Bai G, Wang Y, Hong DM, Jiang JH, Li JX, Hua Y, Wang XY, Chen Y*
- 1236** Efficacy and predictive factors of transarterial chemoembolization combined with lenvatinib plus programmed cell death protein-1 inhibition for unresectable hepatocellular carcinoma  
*Ma KP, Fu JX, Duan F, Wang MQ*
- 1248** Should we perform sigmoidoscopy for colorectal cancer screening in people under 45 years?  
*Leong W, Guo JQ, Ning C, Luo FF, Jiao R, Yang DY*
- 1256** Computed tomography-based radiomics diagnostic approach for differential diagnosis between early- and late-stage pancreatic ductal adenocarcinoma  
*Ren S, Qian LC, Cao YY, Daniels MJ, Song LN, Tian Y, Wang ZQ*
- 1268** Prognostic analysis of related factors of adverse reactions to immunotherapy in advanced gastric cancer and establishment of a nomogram model  
*He XX, Du B, Wu T, Shen H*

**Clinical Trials Study**

- 1281** Safety and efficacy of a programmed cell death 1 inhibitor combined with oxaliplatin plus S-1 in patients with Borrmann large type III and IV gastric cancers  
*Bao ZH, Hu C, Zhang YQ, Yu PC, Wang Y, Xu ZY, Fu HY, Cheng XD*

**Observational Study**

- 1296** Computed tomography radiogenomics: A potential tool for prediction of molecular subtypes in gastric stromal tumor  
*Yin XN, Wang ZH, Zou L, Yang CW, Shen CY, Liu BK, Yin Y, Liu XJ, Zhang B*
- 1309** Application of texture signatures based on multiparameter-magnetic resonance imaging for predicting microvascular invasion in hepatocellular carcinoma: Retrospective study  
*Nong HY, Cen YY, Qin M, Qin WQ, Xie YX, Li L, Liu MR, Ding K*
- 1319** Causal roles of gut microbiota in cholangiocarcinoma etiology suggested by genetic study  
*Chen ZT, Ding CC, Chen KL, Gu YJ, Lu CC, Li QY*
- 1334** Is recovery enhancement after gastric cancer surgery really a safe approach for elderly patients?  
*Li ZW, Luo XJ, Liu F, Liu XR, Shu XP, Tong Y, Lv Q, Liu XY, Zhang W, Peng D*
- 1344** Establishment of a cholangiocarcinoma risk evaluation model based on mucin expression levels  
*Yang CY, Guo LM, Li Y, Wang GX, Tang XW, Zhang QL, Zhang LF, Luo JY*

- 1361** Effectiveness of fecal DNA syndecan-2 methylation testing for detection of colorectal cancer in a high-risk Chinese population

*Luo WF, Jiao YT, Lin XL, Zhao Y, Wang SB, Shen J, Deng J, Ye YF, Han ZP, Xie FM, He JH, Wan Y*

#### Clinical and Translational Research

- 1374** Clinical and socioeconomic determinants of survival in biliary tract adenocarcinomas

*Sahyoun L, Chen K, Tsay C, Chen G, Protiva P*

- 1384** Risk factors, prognostic factors, and nomograms for distant metastasis in patients with diagnosed duodenal cancer: A population-based study

*Shang JR, Xu CY, Zhai XX, Xu Z, Qian J*

- 1421** NOX4 promotes tumor progression through the MAPK-MEK1/2-ERK1/2 axis in colorectal cancer

*Xu YJ, Huo YC, Zhao QT, Liu JY, Tian YJ, Yang LL, Zhang Y*

#### Basic Study

- 1437** Curcumin inhibits the growth and invasion of gastric cancer by regulating long noncoding RNA AC022424.2

*Wang BS, Zhang CL, Cui X, Li Q, Yang L, He ZY, Yang Z, Zeng MM, Cao N*

- 1453** MicroRNA-298 determines the radio-resistance of colorectal cancer cells by directly targeting human dual-specificity tyrosine(Y)-regulated kinase 1A

*Shen MZ, Zhang Y, Wu F, Shen MZ, Liang JL, Zhang XL, Liu XJ, Li XS, Wang RS*

- 1465** Human  $\beta$ -defensin-1 affects the mammalian target of rapamycin pathway and autophagy in colon cancer cells through long non-coding RNA TCONS\_00014506

*Zhao YX, Cui Y, Li XH, Yang WH, An SX, Cui JX, Zhang MY, Lu JK, Zhang X, Wang XM, Bao LL, Zhao PW*

- 1479** FAM53B promotes pancreatic ductal adenocarcinoma metastasis by regulating macrophage M2 polarization

*Pei XZ, Cai M, Jiang DW, Chen SH, Wang QQ, Lu HM, Lu YF*

- 1500** Transcriptome sequencing reveals novel biomarkers and immune cell infiltration in esophageal tumorigenesis

*Sun JR, Chen DM, Huang R, Wang RT, Jia LQ*

- 1514** Construction of CDKN2A-related competitive endogenous RNA network and identification of GAS5 as a prognostic indicator for hepatocellular carcinoma

*Pan Y, Zhang YR, Wang LY, Wu LN, Ma YQ, Fang Z, Li SB*

- 1532** Two missense *STK11* gene variations impaired LKB1/adenosine monophosphate-activated protein kinase signaling in Peutz-Jeghers syndrome

*Liu J, Zeng SC, Wang A, Cheng HY, Zhang QJ, Lu GX*

- 1547** Long noncoding RNAs HAND2-AS1 ultrasound microbubbles suppress hepatocellular carcinoma progression by regulating the miR-873-5p/tissue inhibitor of matrix metalloproteinase-2 axis

*Zou Q, Wang HW, Di XL, Li Y, Gao H*

- 1564** Upregulated lncRNA PRNT promotes progression and oxaliplatin resistance of colorectal cancer cells by regulating HIPK2 transcription

*Li SN, Yang S, Wang HQ, Hui TL, Cheng M, Zhang X, Li BK, Wang GY*

**SYSTEMATIC REVIEWS**

- 1578** Prognosis value of heat-shock proteins in esophageal and esophagogastric cancer: A systematic review and meta-analysis

*Nakamura ET, Park A, Pereira MA, Kikawa D, Tustumi F*

- 1596** Risk factors for hepatocellular carcinoma associated with hepatitis C genotype 3 infection: A systematic review

*Farooq HZ, James M, Abbott J, Oyibo P, Divall P, Choudhry N, Foster GR*

**META-ANALYSIS**

- 1613** Effectiveness and tolerability of programmed cell death protein-1 inhibitor + chemotherapy compared to chemotherapy for upper gastrointestinal tract cancers

*Zhang XM, Yang T, Xu YY, Li BZ, Shen W, Hu WQ, Yan CW, Zong L*

- 1626** Success rate of current human-derived gastric cancer organoids establishment and influencing factors: A systematic review and meta-analysis

*Jiang KL, Wang XX, Liu XJ, Guo LK, Chen YQ, Jia QL, Yang KM, Ling JH*

**CASE REPORT**

- 1647** Pathologically successful conversion hepatectomy for advanced giant hepatocellular carcinoma after multidisciplinary therapy: A case report and review of literature

*Chu JH, Huang LY, Wang YR, Li J, Han SL, Xi H, Gao WX, Cui YY, Qian MP*

- 1660** Clinical pathological characteristics of “crawling-type” gastric adenocarcinoma cancer: A case report

*Xu YW, Song Y, Tian J, Zhang BC, Yang YS, Wang J*

- 1668** Primary pancreatic peripheral T-cell lymphoma: A case report

*Bai YL, Wang LJ, Luo H, Cui YB, Xu JH, Nan HJ, Yang PY, Niu JW, Shi MY*

**ABOUT COVER**

Peer Reviewer of *World Journal of Gastrointestinal Oncology*, Lie Zheng, Director, Professor, Department of Gastroenterology, Shaanxi Provincial Hospital of Traditional Chinese Medicine, Xi'an 730000, Shaanxi Province, China. xinliwen696@126.com

**AIMS AND SCOPE**

The primary aim of *World Journal of Gastrointestinal Oncology (WJGO, World J Gastrointest Oncol)* is to provide scholars and readers from various fields of gastrointestinal oncology with a platform to publish high-quality basic and clinical research articles and communicate their research findings online.

*WJGO* mainly publishes articles reporting research results and findings obtained in the field of gastrointestinal oncology and covering a wide range of topics including liver cell adenoma, gastric neoplasms, appendiceal neoplasms, biliary tract neoplasms, hepatocellular carcinoma, pancreatic carcinoma, cecal neoplasms, colonic neoplasms, colorectal neoplasms, duodenal neoplasms, esophageal neoplasms, gallbladder neoplasms, *etc.*

**INDEXING/ABSTRACTING**

The *WJGO* is now abstracted and indexed in PubMed, PubMed Central, Science Citation Index Expanded (SCIE, also known as SciSearch®), Journal Citation Reports/Science Edition, Scopus, Reference Citation Analysis, China Science and Technology Journal Database, and Superstar Journals Database. The 2023 edition of Journal Citation Reports® cites the 2022 impact factor (IF) for *WJGO* as 3.0; IF without journal self cites: 2.9; 5-year IF: 3.0; Journal Citation Indicator: 0.49; Ranking: 157 among 241 journals in oncology; Quartile category: Q3; Ranking: 58 among 93 journals in gastroenterology and hepatology; and Quartile category: Q3. The *WJGO*'s CiteScore for 2022 is 4.1 and Scopus CiteScore rank 2022: Gastroenterology is 71/149; Oncology is 197/366.

**RESPONSIBLE EDITORS FOR THIS ISSUE**

**Production Editor:** *Xiang-Di Zhang*; **Production Department Director:** *Xiang Li*; **Cover Editor:** *Jia-Ru Fan*.

**NAME OF JOURNAL**

*World Journal of Gastrointestinal Oncology*

**ISSN**

ISSN 1948-5204 (online)

**LAUNCH DATE**

February 15, 2009

**FREQUENCY**

Monthly

**EDITORS-IN-CHIEF**

Monjur Ahmed, Florin Burada

**EDITORIAL BOARD MEMBERS**

<https://www.wjgnet.com/1948-5204/editorialboard.htm>

**PUBLICATION DATE**

April 15, 2024

**COPYRIGHT**

© 2024 Baishideng Publishing Group Inc

**INSTRUCTIONS TO AUTHORS**

<https://www.wjgnet.com/bpg/gerinfo/204>

**GUIDELINES FOR ETHICS DOCUMENTS**

<https://www.wjgnet.com/bpg/GerInfo/287>

**GUIDELINES FOR NON-NATIVE SPEAKERS OF ENGLISH**

<https://www.wjgnet.com/bpg/gerinfo/240>

**PUBLICATION ETHICS**

<https://www.wjgnet.com/bpg/GerInfo/288>

**PUBLICATION MISCONDUCT**

<https://www.wjgnet.com/bpg/gerinfo/208>

**ARTICLE PROCESSING CHARGE**

<https://www.wjgnet.com/bpg/gerinfo/242>

**STEPS FOR SUBMITTING MANUSCRIPTS**

<https://www.wjgnet.com/bpg/GerInfo/239>

**ONLINE SUBMISSION**

<https://www.f6publishing.com>



Observational Study

## Establishment of a cholangiocarcinoma risk evaluation model based on mucin expression levels

Chun-Yuan Yang, Li-Mei Guo, Yang Li, Guang-Xi Wang, Xiao-Wei Tang, Qiu-Lu Zhang, Ling-Fu Zhang, Jian-Yuan Luo

**Specialty type:** Oncology

**Provenance and peer review:**

Unsolicited article; Externally peer reviewed.

**Peer-review model:** Single blind

**Peer-review report's scientific quality classification**

Grade A (Excellent): 0  
Grade B (Very good): B  
Grade C (Good): 0  
Grade D (Fair): 0  
Grade E (Poor): 0

**P-Reviewer:** Ueda H, Japan

**Received:** December 20, 2023

**Peer-review started:** December 20, 2023

**First decision:** December 27, 2023

**Revised:** January 9, 2024

**Accepted:** February 25, 2024

**Article in press:** February 25, 2024

**Published online:** April 15, 2024



**Chun-Yuan Yang, Li-Mei Guo, Yang Li, Guang-Xi Wang, Xiao-Wei Tang, Qiu-Lu Zhang,** Department of Pathology, Institute of Systems Biomedicine, School of Basic Medical Sciences Peking University, Peking University Third Hospital, Peking University Health Science Center, Beijing 100191, China

**Ling-Fu Zhang,** Department of General Surgery, Peking University Third Hospital, Beijing 100191, China

**Jian-Yuan Luo,** Department of Medical Genetics, Department of Biochemistry and Biophysics, School of Basic Medical Sciences Peking University, Peking University Health Science Center, Beijing 100191, China

**Corresponding author:** Li-Mei Guo, MD, Doctor, Professor, Department of Pathology, Institute of Systems Biomedicine, School of Basic Medical Sciences Peking University, Peking University Third Hospital, Peking University Health Science Center, No. 38 Xueyuan Road, Haidian District, Beijing 100191, China. [guolimei@bjmu.edu.cn](mailto:guolimei@bjmu.edu.cn)

### Abstract

#### BACKGROUND

Cholangiocarcinoma (CCA) is a highly malignant cancer, characterized by frequent mucin overexpression. *MUC1* has been identified as a critical oncogene in the progression of CCA. However, the comprehensive understanding of how the mucin family influences CCA progression and prognosis is still incomplete.

#### AIM

To investigate the functions of mucins on the progression of CCA and to establish a risk evaluation formula for stratifying CCA patients.

#### METHODS

Single-cell RNA sequencing data from 14 CCA samples were employed for elucidating the roles of mucins, complemented by bioinformatic analyses. Subsequent validations were conducted through spatial transcriptomics and immunohistochemistry. The construction of a risk evaluation model utilized the least absolute shrinkage and selection operator regression algorithm, which was further confirmed by independent cohorts and diverse data types.

#### RESULTS

CCA tumor cells with elevated levels of *MUC1* and *MUC4* showed activated nucleotide metabolic pathways and increased invasiveness. *MUC5AC*-high cells were found to promote CCA progression through WNT signaling. *MUC5B*-high cells exhibited robust cellular oxidation activities, leading to resistance against antitumoral treatments. *MUC13*-high cells were observed to secrete chemokines, recruiting and transforming macrophages into the M2-polarized state, thereby suppressing antitumor immunity. *MUC16*-high cells were found to promote tumor progression through interleukin-1/nuclear factor kappa-light-chain-enhancer of activated B cells signaling upon interaction with neutrophils. Utilizing the expression levels of these mucins, a risk factor evaluation formula for CCA was developed and validated across multiple cohorts. CCA samples with higher risk factors exhibited stronger metastatic potential, chemotherapy resistance, and poorer prognosis.

## CONCLUSION

Our study elucidates the functional mechanisms through which mucins contribute to CCA development, and provides tools for risk stratification in CCA.

**Key Words:** Mucin; Cholangiocarcinoma; Single-cell RNA sequencing; Spatial transcriptomics; Prognosis

©The Author(s) 2024. Published by Baishideng Publishing Group Inc. All rights reserved.

**Core Tip:** In this study, we have conducted a comprehensive investigation of mucins in cholangiocarcinoma (CCA) using a combination of bioinformatics analysis, including single-cell RNA sequencing and spatial transcriptomics, along with experimental validations. Our findings highlight the significant roles of *MUC1*, *MUC4*, and *MUC5B* in CCA metabolism, contributing to tumor progression and therapy resistance. Additionally, *MUC5AC* has been identified as a regulator of CCA invasiveness through the WNT signaling. *MUC13* and *MUC16* are found to play critical roles in tumor-immune interactions, regulating antitumoral immune defense. The collect impact of these mucins enables the development of a CCA prognosis evaluation model that effectively predicts tumor malignancy, treatment effectiveness, and prognosis in CCA cases.

**Citation:** Yang CY, Guo LM, Li Y, Wang GX, Tang XW, Zhang QL, Zhang LF, Luo JY. Establishment of a cholangiocarcinoma risk evaluation model based on mucin expression levels. *World J Gastrointest Oncol* 2024; 16(4): 1344-1360

**URL:** <https://www.wjgnet.com/1948-5204/full/v16/i4/1344.htm>

**DOI:** <https://dx.doi.org/10.4251/wjgo.v16.i4.1344>

## INTRODUCTION

Cholangiocarcinoma (CCA) is the second most common malignant liver cancer and has exhibited a rising incidence and mortality trend over the past four decades[1,2]. CCA is categorized into intrahepatic CCA (iCCA), perihilar CCA (pCCA) and distal CCA based on the primary anatomic region, among which the former two subtypes constitute approximately 70%-80% of cases[3]. The majority of patients are diagnosed at an advanced stage, limiting treatment options[4]. For patients who are ineligible for surgical resection, chemotherapy, particularly gemcitabine and cisplatin combination, becomes their primary choice, however, the median survival period remains less than one year[5]. While molecularly targeted therapies show promising antitumor effects[6], patients suitable for these targeted therapies are relatively scarce.

Histopathologically, CCA is classified into two primary subgroups: the mucin-producing subgroup and the nonmucin-producing subgroup[7]. Consequently, mucins play pivotal roles in CCA development. Mucins, a family of proteins widely distributed on the epithelial surface of various organs, serve essential functions in lubrication and defense against toxins and infections[8]. In addition to their physiological roles, mucins play important roles in pathological conditions, including cancer. Abnormal expression and distribution of mucins are found in various cancer types, such as lung cancer, breast cancer, pancreatic cancer, colorectal cancer, gastric cancer, liver cancer, and ovarian cancer[9,10]. Numerous studies have explored the mechanisms of *MUC1* in tumorigenesis, implicating multiple signaling pathways, including the Ras,  $\beta$ -catenin, TP53, nuclear factor kappa-light-chain-enhancer of activated B cells (NF- $\kappa$ B), transforming growth factor  $\beta$ , and vascular endothelial growth factor[10]. However, clinical trials investigating *MUC1* have not demonstrated significant treatment effects compared to those in control groups[11,12], highlighting the need to systematically target multiple mucins.

In recent decades, single-cell RNA sequencing (scRNA-seq) has revolutionized cancer research, leading to remarkable milestones. The application of scRNA-seq to CCA has revealed intratumor heterogeneity at the single-cell level[13], identified new markers for different CCA subtypes[14], characterized sub-clusters of cancer-associated fibroblasts[15], and elucidated intercellular crosstalk within the tumor microenvironment (TME)[16]. Nevertheless, mucin functions and the characteristics of mucin-expressing CCA cells have not been previously explored at single-cell resolution. In this study, we comprehensively analyzed the scRNA-seq data from 14 human CCA samples, including 13 iCCA patients and one pCCA patient, to determine the mechanisms of various mucins, specifically *MUC1*, *MUC4*, *MUC5AC*, *MUC5B*, *MUC13*, and *MUC16*, in promoting CCA progression. The mucin-based CCA patient stratification system provides a new dimension for CCA prognosis prediction, and offers potential strategies for CCA treatment.

## MATERIALS AND METHODS

### Single-cell RNA sequencing data analysis

Our scRNA-seq data of CCA samples were sourced from the gene expression omnibus database (GSE154170, GSE138709, GSE142784, and GSE125449). After selecting samples from treatment-naïve CCA patients, we integrated these data into a unified dataset using R package Harmony. Following normalization, nonlinear dimensionality reduction was applied to reduce the dimensionality of data. Subsequently, cell clustering was performed using the standard methods suggested by satijalab (<https://satijalab.org/seurat/>). This resulted in the identification of six cell types. Cells from normal tissues and hepatocytes were filtered out, leaving only CCA tumor cells for the functional evaluation of mucins. Myeloid cells were performed under the same methodology.

### Transcription factor analysis

The R package SCENIC (<http://scenic.aertslab.org>) was utilized to identify putative transcription factors and regulons of *MUC1*-high and *MUC1*-low cells[17]. Marker regulons of *MUC1*-high cells were identified by comparing different regulons between *MUC1*-high and *MUC1*-low cells using FindAllMarker function.

### Gene set enrichment analysis

Our gene set enrichment analysis (GSEA) was conducted using the R package fgsea. The oncogenic and metabolic pathways involved in our study were obtained from MSigDB (<http://www.gseamsigdb.org/gsea/msigdb>). The normalized enrichment score value was calculated by the difference enrichment score between *MUC1*-high and *MUC1*-low cells, *MUC5AC*-high vs *MUC5AC*-low cells, *MUC5B*-high vs *MUC5B*-low cells, *MUC13*-high cells vs *MUC13*-low cells, and *MUC16*-high cells vs *MUC16*-low cells.

### Gene set variation analysis

Comprehensive analyses of 70 metabolic signaling pathways were performed using gene set variation analysis (GSVA) with the R package GSVA. The 70 metabolic pathways were collected based on a previous article[18]. After calculation the rank values of each gene in each geneset, the rank value was constrained from -3 to 3 to avoid extreme values. Subsequently, the rank values of each cluster of cells were normalized to their mean value to generate the heatmap.

### Spatial transcriptomics data analysis

Spatial transcriptomics (ST) data were obtained from a published liver cancer dataset (cohort 9, [Supplementary Table 1](#)), which included hepatocellular carcinoma samples, CCA samples, and combined hepatocellular-CCA[19]. We selected the cHC-1T sample, exhibiting clear CCA histological features, for functional detection of *MUC1* and *MUC5B*. ST data analysis followed the guidelines provided by satijala ([https://satijalab.org/seurat/articles/spatial\\_vignette](https://satijalab.org/seurat/articles/spatial_vignette)).

### Gene expression correlation analyses

Expression data of mucins and *WNT7B*, *ALDH1A1*, *UCP2*, *CSF3R*, *NFKB1*, *NFKB2*, *RELA* were obtained from a previously reported dataset[20]. Correlations between mucins and these genes was evaluated using the R package ggplot2. The significance of these correlations was determined by Pearson's correlation analysis ( $P \leq 0.05$ ).

### Cell interaction analysis

Cellular interaction network analysis was performed using the R package CellChat (<http://www.cellchat.org/>)[21]. When analyzing interactions between CCA sub-cluster and other cell types in TME, we randomly selected 1000 cells in each TME cell partitions, including lymphocytes, fibroblasts, endothelial cells, and myeloid cells.

### CCA risk factor model establishment

To assess CCA prognosis based on mucins, we applied the least absolute shrinkage and selection operator (LASSO) algorithm on the RNA levels of *MUC1*, *MUC13*, *MUC16*, *MUC4*, *MUC5AC*, and *MUC5B* by R package glmnet. RNA levels were normalized using the trans per million method. The CCA risk score was then established as follows: risk score = sum (each MUC gene expression × corresponding coefficient). The coefficient for *MUC1*, *MUC13*, *MUC16*, *MUC4*, *MUC5AC*, and *MUC5B* are 0.0297, 0.0460, 0.1217, 0.0574, 0.0501, and 0.0657, respectively. Subsequently, the CCA patients were stratified into high-risk and low-risk groups.

### CCA patient survival analysis

The patient survival information, along with corresponding RNA-seq data and protein expression levels of tumor samples, were obtained from cohort 2 and cohort 10. The correlation between CCA patient survival, individual mucin expression (including *MUC1*, *MUC4*, *MUC5AC*, *MUC5B*, *MUC13*, and *MUC16*), and risk factors was assessed using the log-rank (Mantel-Cox) test.

### Independent CCA samples and double staining immunohistochemistry

Validation of mucin functions was conducted using primary CCA samples resected at Peking University Third Hospital. Our study was approved by the Ethics Committee of Peking University Third Hospital. All research was conducted in accordance with both the Declarations of Helsinki and Istanbul. All patients were informed and kept anonymous.

Formalin-fixed and paraffin-embedded 4- $\mu$ m tissue sections were used for immunohistochemistry (IHC) staining. Briefly, sections were dehydrated with graded concentrations of ethanol and immersed in 3% hydrogen peroxide for 15 min. Antigen retrieval was performed by heating for 2 min in a pressure cooker using 0.01 M citrate buffer (pH 6.0). Sections were then incubated with primary antibodies against *MUC13* (Abcam, Cat ab235450), *MUC16* (Origene, Cat ZM-0019), CD163 (Origene, Cat ZM-0428), and CD66b (Abcam, Cat ab300122) at 4 °C overnight. The GTVision™ Double Staining Detection System (Dako, Cat GK700110) was used for the secondary antibody and 3,3-diaminobenzidine/hydrogen peroxide was used as the chromogen. Substitution of the primary antibody with phosphate-buffered saline was used as a negative control.

### Statistics

Comparisons of gene expression levels between tumor and non-tumoral normal tissue were performed using paired or unpaired student's *t*-test. The signaling pathway enrichment analysis was performed using Fisher's exact test. The GSEA was performed using Wilcoxon-Mann-Whitney test. The GSVA was performed using Kolmogorov-Smirnov like random walk test. Patient survival analysis was performed using the log-rank (Mantel-Cox) test. Correlation analyses of mucin expression levels and CCA pathological phenotypes were subjected to Chi-square analysis. All analyses were performed by R or GraphPad Prism. Differences were regarded significant when  $P < 0.05$ .

## RESULTS

### Clinical significance and heterogeneity of mucins in CCA

Despite previous reports suggesting the potential diagnostic roles of mucins in CCA [10,22,23], systematic evaluation of all mucins in CCA is lacking. This study introduced multiple clinical cohorts to assess the clinical relevance of mucins in CCA. Cohort 1 (Supplementary Table 1) was sourced from the CCA dataset in The Cancer Genome Atlas database. Among the 20 mucin-encoding genes, many mucins exhibited significantly higher expression levels in tumor tissues than in normal tissues (Supplementary Figure 1A), emphasizing the critical functions of mucins in CCA development. Notably, elevated expression levels of *MUC1*, *MUC4*, *MUC5AC*, *MUC5B*, *MUC13*, and *MUC16* were found to predict poor CCA prognosis in cohort 2 (Supplementary Table 1) [24] (Figure 1A). Therefore, we focused on the functional evaluation of these mucins in this study. Two additional independent CCA cohorts (cohorts 3 and 4, Supplementary Table 1) further validated the upregulation of the abovementioned mucins in both unpaired [25] (Supplementary Figure 1B) and paired [26] (Supplementary Figure 1C) CCA samples. However, given the heterogeneity of CCA, a detailed investigation of mucins at the single-cell level is imperative.

To evaluate mucin heterogeneity at the single-cell level, we combined the scRNA-seq data from four independent datasets (cohorts 5, 6, 7, and 8 in Supplementary Table 1) [15,16,27], and reanalyzed the integrated data. The integrated dataset comprised 51810 single cells from 14 patients (Supplementary Table 2), and was classified into six cell types, namely cycling cells, dying cells, epithelial cells, lymphocytes, myeloid cells, and stromal cells (Supplementary Figure 2A). The marker gene expression levels and proportions further confirmed the annotation of these cell types (Supplementary Figure 2B). For quality control, we examined the batch effect of our data integration by evaluating the distribution features of cells from different patients. The result indicated a fine mixture of cells from different patients, suggesting low batch effects (Supplementary Figure 2C). Additionally, the observed differences in gene expression between cells from normal regions and tumor regions (Supplementary Figure 2D) suggested the occurrence of transcriptomic remodeling during CCA development.

To evaluate the functions of mucins (*MUC1*, *MUC4*, *MUC5AC*, *MUC5B*, *MUC13*, and *MUC16*) in CCA at the single-cell level, we extracted tumor cells from the integrated data. Re-clustering of the tumor cells resulted in the formation of 29 sub-clusters, designated C1 to C29 (Figure 1B). The marker gene expression for each sub-cluster is shown in Supplementary Figure 3. Notably, the detection of mucin expression revealed many sub-clusters expressing high levels of the *MUC1* and *MUC4* genes, including C1, C4, C5, C6, C9, C12, C13, C14, C15, C22, C23, C25, C27 and C28 (Figure 1C). Therefore, we examined *MUC1* and *MUC4* collectively afterward. In contrast, *MUC5AC*, *MUC5B*, *MUC13* and *MUC16* exhibited relatively unique distribution patterns (Figure 1C). *MUC5AC* was enriched in C23. *MUC5B* was enriched in C22 and C27. *MUC13* was enriched in C23 and C29. *MUC16* was enriched in C20 and C28. Subsequently, functional analyses were performed on *MUC1*, *MUC5AC*, *MUC5B*, *MUC13*, and *MUC16*, independently.

### Selective activation of nucleotide metabolism in *MUC1*-high CCA cells

To elucidate the functions of *MUC1* in CCA, we integrated sub-clusters C1, C4, C5, C6, C9, C12, C13, C14, C15, C22, C23, C25, C27, and C28 into *MUC1*-high subgroup, and integrated the remaining sub-clusters into *MUC1*-low subgroup. Next, we compared the gene expression profiles between *MUC1*-high cells and *MUC1*-low cells, and identified differentially expressed genes (DEGs). Pathway enrichment analysis of these DEGs revealed pronounced activation of metabolic pathways in *MUC1*-high cells (Supplementary Figure 4A). To determine the metabolic characteristics of *MUC1*-high cells, we employed a 70-pathway metabolic analysis panel, which demonstrated heightened activation of pathways related to nucleotide, energy, amino acid, and detoxification metabolism in *MUC1*-high cells (Figure 2A). Among these metabolic processes, nucleotide metabolism exhibited a prominent role, as indicated by the identification of numerous pathways (Figure 2A, highlighted in red). Independent analyses of nucleotide metabolic pathways (Supplementary Figure 4B-D) and nucleotide excision repair (Supplementary Figure 4E and F) further validated the distinctive features of *MUC1*-high cells. Moreover, compared with *MUC1*-low cells, *MUC1*-high cells displayed elevated expression levels of RNA polymerase components and DNA repair regulators (Supplementary Figure 4G).

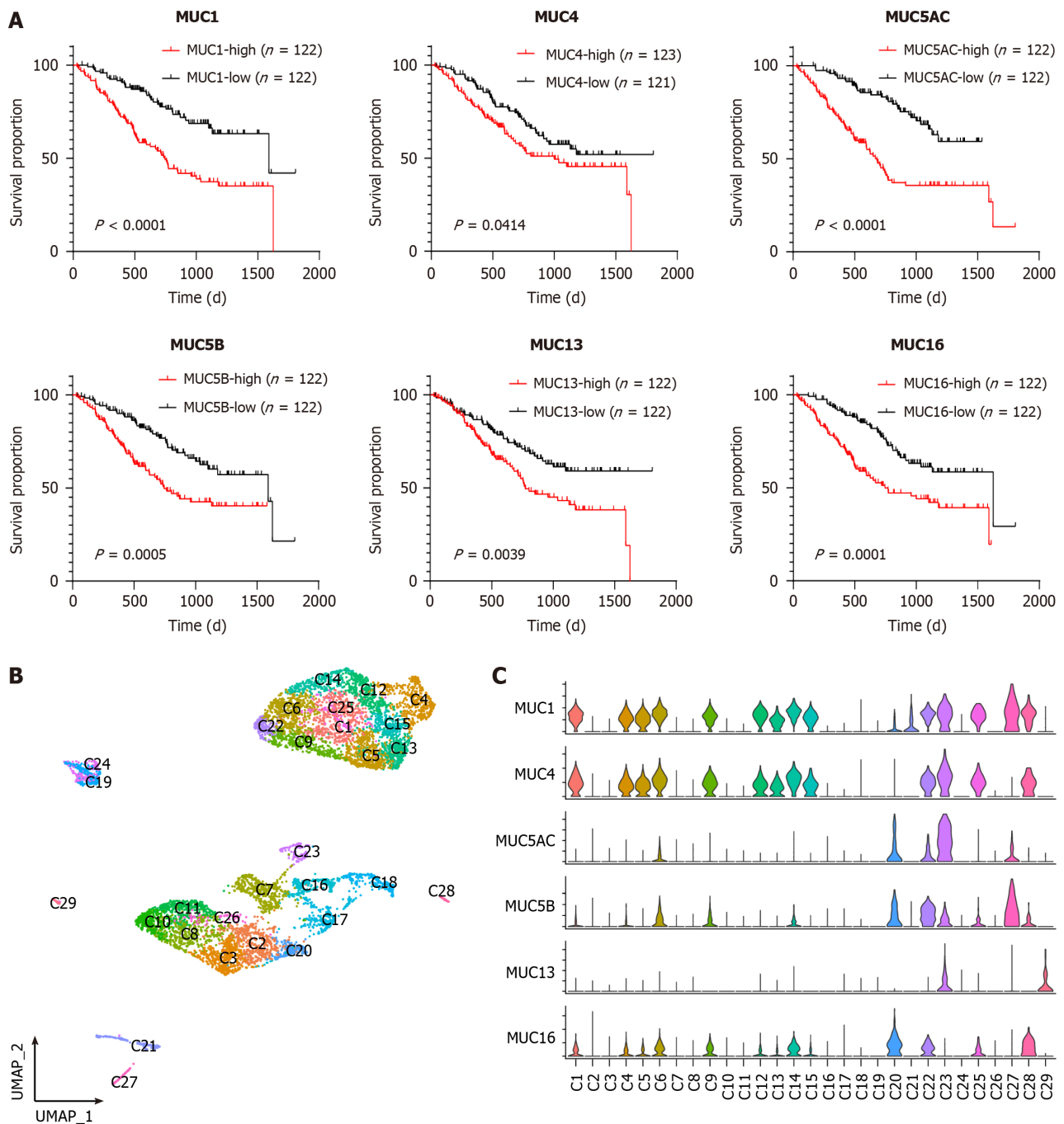


**Figure 1 Clinical significance and heterogeneity of mucins in cholangiocarcinoma.** A: Survival curves generated using cohort 2 data illustrating the relationship between cholangiocarcinoma (CCA) patient survival and the mRNA levels of mucins; B: Uniform manifold approximation and projection plot visually representing the tumor cell sub-clusters within the integrated CCA dataset; C: Violin plots depicting of the relative gene expression levels of *MUC1*, *MUC4*, *MUC5AC*, *MUC5B*, *MUC13*, and *MUC16* in CCA tumor sub-clusters.

To unravel the mechanisms underlying the observed metabolic characteristics of *MUC1*-high cells, we analyzed the transcription factor expression in these cells. Compared with *MUC1*-low cells, *MUC1*-high cells exhibited uniquely higher expression levels of *NFIC* and *FOSL1* (Figure 2B). *FOSL1* is known to regulate the expression of another transcription factor, *HMGA1*[28], which was found to play important roles in nucleotide metabolism[29,30]. Examination of the co-expression patterns of *FOSL1*, *HMGA1*, and *MUC1* in both scRNA-seq (Supplementary Figure 4H) and ST (cohort 9, Supplementary Table 1) (Figure 2C) data indicated significant co-expression. Importantly, both *FOSL1* and *HMGA1* are implicated tumor progression[30,31]. GSEA confirmed the enhanced proliferation and metastasis characteristics of *MUC1*-high cells compared to *MUC1*-low cells (Figure 2D and E). Taken together, our analyses reveal the activation of nucleotide metabolism and high invasion status of *MUC1*-high cells.

**Activation of the WNT signaling pathway in *MUC5AC*-high CCA cells**

Given the substantial expression of *MUC5AC* in cluster C23 (Figure 1C), we defined C23 cells as *MUC5AC*-high cells, and the remaining sub-clusters as *MUC5AC*-low cells. Analysis of DEGs in the *MUC5AC*-high cluster *vs* the *MUC5AC*-low

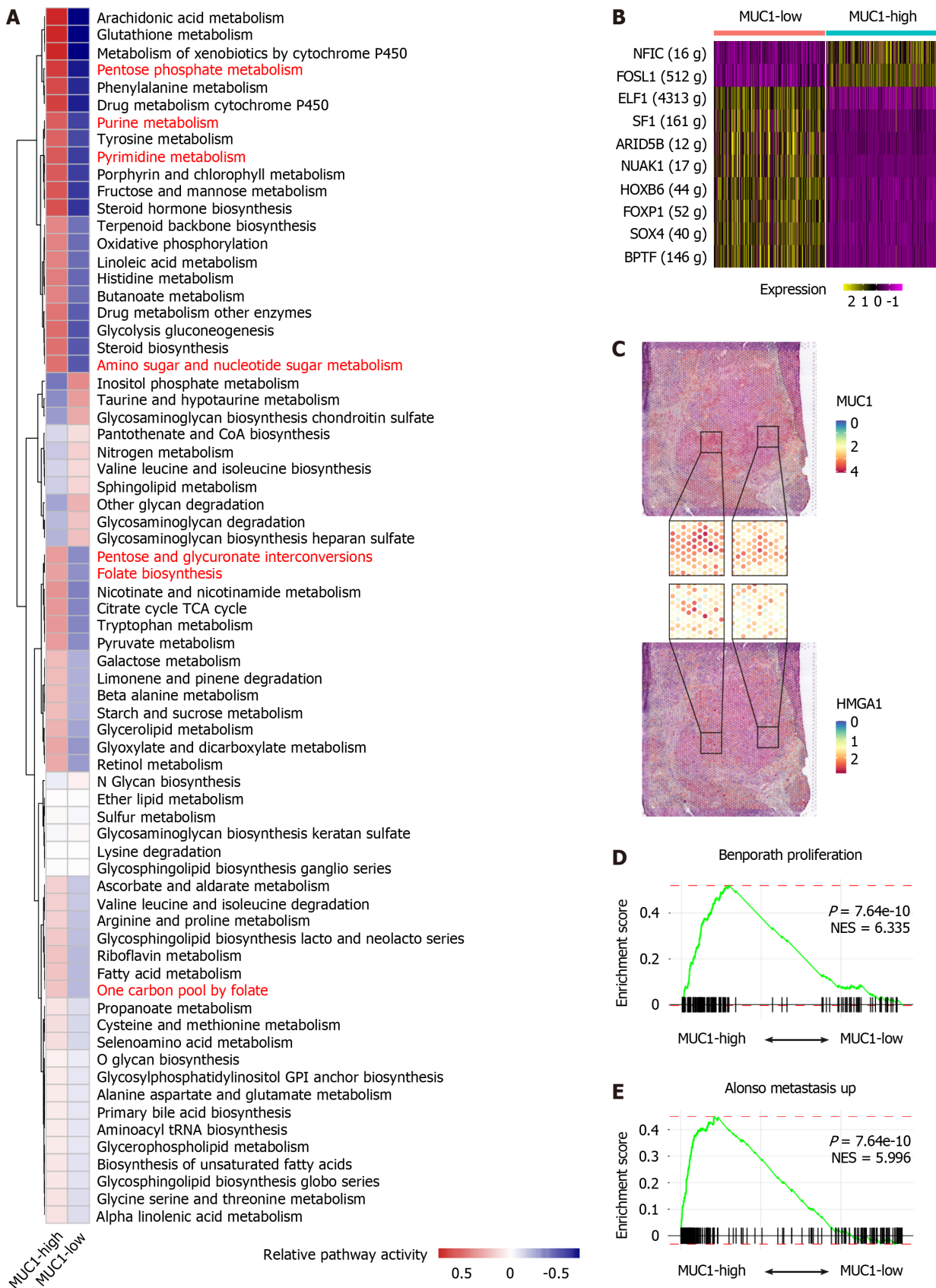


**Figure 2 Activated nucleotide metabolic signaling and higher malignant characteristics in *MUC1*-high tumor cells of cholangiocarcinoma.** A: Heatmap showing the activity of metabolic signaling pathways in *MUC1*-high vs *MUC1*-low cells; B: Heatmap showing the different expression levels of transcription factors in *MUC1*-high cells vs *MUC1*-low cells; C: Distribution of *MUC1* and *HMGA1* in the spatial transcriptomics (ST) slide. Zoomed in portions of the ST chip (middle) showing multiple areas of co-localization; D and E: Gene set enrichment analysis plots showing the enrichment of genes from *MUC1*-high cells (left) vs *MUC1*-low cells (right) in cell proliferation and metastasis signaling pathways. The *P* values and normalized enrichment score are indicated on the plots.

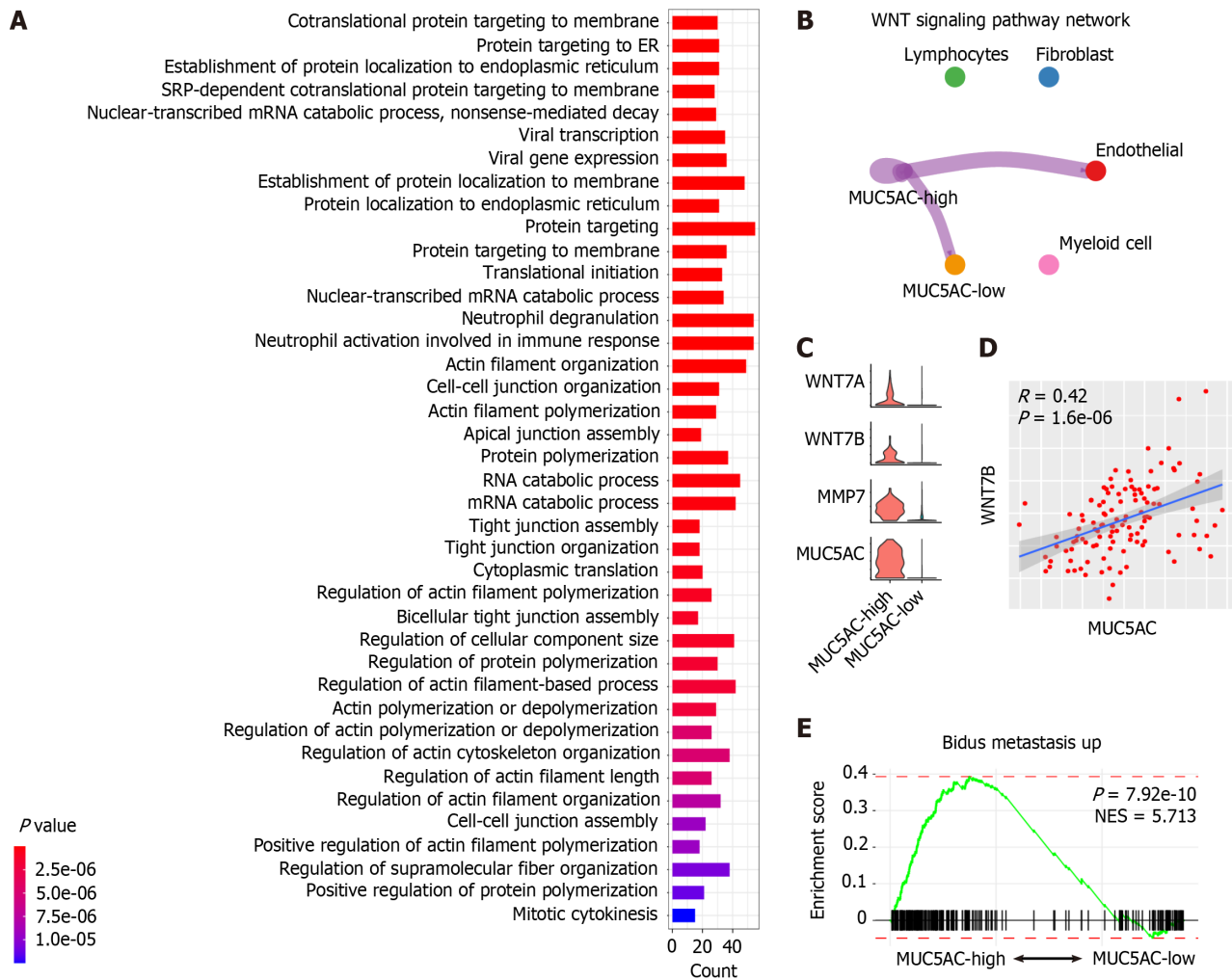


**Figure 3** WNT signaling and metabolic phenotypes in *MUC5AC*-high tumor cells of cholangiocarcinoma. **A**: Top 40 enriched signaling pathways of the differentially expressed genes in *MUC5AC*-high cells; **B**: Relative activity of the WNT signaling pathway among *MUC5AC*-high, *MUC5AC*-low, myeloid cells, endothelial cells, fibroblasts, and lymphocytes; **C**: Violin plots showing relative expression levels of *WNT7A*, *WNT7B*, and *MMP7* in *MUC5AC*-high vs *MUC5AC*-low cholangiocarcinoma (CCA) cells; **D**: Correlation analysis between the expression of *MUC5AC* and *WNT7B* in CCA tumor samples from cohort 10; **E**: Gene set enrichment analysis plot showing the enrichment of genes from the *MUC5AC*-high (left) and *MUC5AC*-low (right) cells in tumor metastasis signaling pathway. The *P* value and normalized enrichment score are indicated on the plot.

cluster revealed enrichment of cell-cell junctions and actin-related cellular mobility pathways (Figure 3A), implicating *MUC5AC* in CCA metastasis. Cellular interaction analysis using CellChat demonstrated activation of the WNT signaling pathway in *MUC5AC*-high cells (Figure 3B). Given the tumor-promoting functions of the WNT pathway[32], we examined the expression of WNT ligands, including *WNT7A* and *WNT7B*, as well as the WNT target gene *MMP7*[33], in *MUC5AC*-high and *MUC5AC*-low cells (Figure 3C). Co-expression analysis of *MUC5B* and *WNT7B* in an independent CCA cohort (cohort 10, Supplementary Table 1) confirmed a significant correlation (Figure 3D), supporting the activation of the WNT signaling pathway in *MUC5AC*-high CCA cells. Subsequent GSEA further verified the metastasis-promoting role of *MUC5AC*-high cells (Figure 3E and Supplementary Figure 5).

### Cellular oxidation and detoxification characteristics of *MUC5B*-high cells

To unravel the functions of *MUC5B* in CCA, we stratified CCA cells based on *MUC5B* expression level in the scRNA-seq data. Combining sub-clusters C22 and C27 as the *MUC5B*-high subgroup (Figure 1C), the remaining sub-clusters formed the *MUC5B*-low subgroup. Comparative analysis revealed that the DEGs of *MUC5B*-high cells were highly enriched in cellular oxidation and detoxification pathways (Figure 4A). Additional cellular oxidation pathways from independent datasets further confirmed the active oxidation status of *MUC5B*-high cells (Figure 4B). Furthermore, the scRNA-seq data revealed that *GSTA1*, *GSTA2*, *ALDH1A1*, *ALDH2*, and *UCP2* were highly co-expressed with *MUC5B* (Figure 4C). These genes not only participate in detoxification processes, but also indicate antitumor treatment resistance and poor prognosis in cancer patients[34-37]. Chemotherapy sensitivity analysis of *MUC5B*-high cells demonstrated that *MUC5B*-high cells exhibited significantly greater resistance to antitumor drugs than *MUC5B*-low cells did (Figure 4D, and Supplementary Figure 6). Furthermore, *in-situ* co-expression of *MUC5B* and *GSTA1* was observed in the ST data (Figure 4E). Co-expression of *MUC5B* with *ALDH1A1* or *UCP2* was further confirmed in cohort 10 (Figure 4F). Collectively, these data reveal the active oxidation state and chemotherapy resistance characteristics of *MUC5B*-high cells.

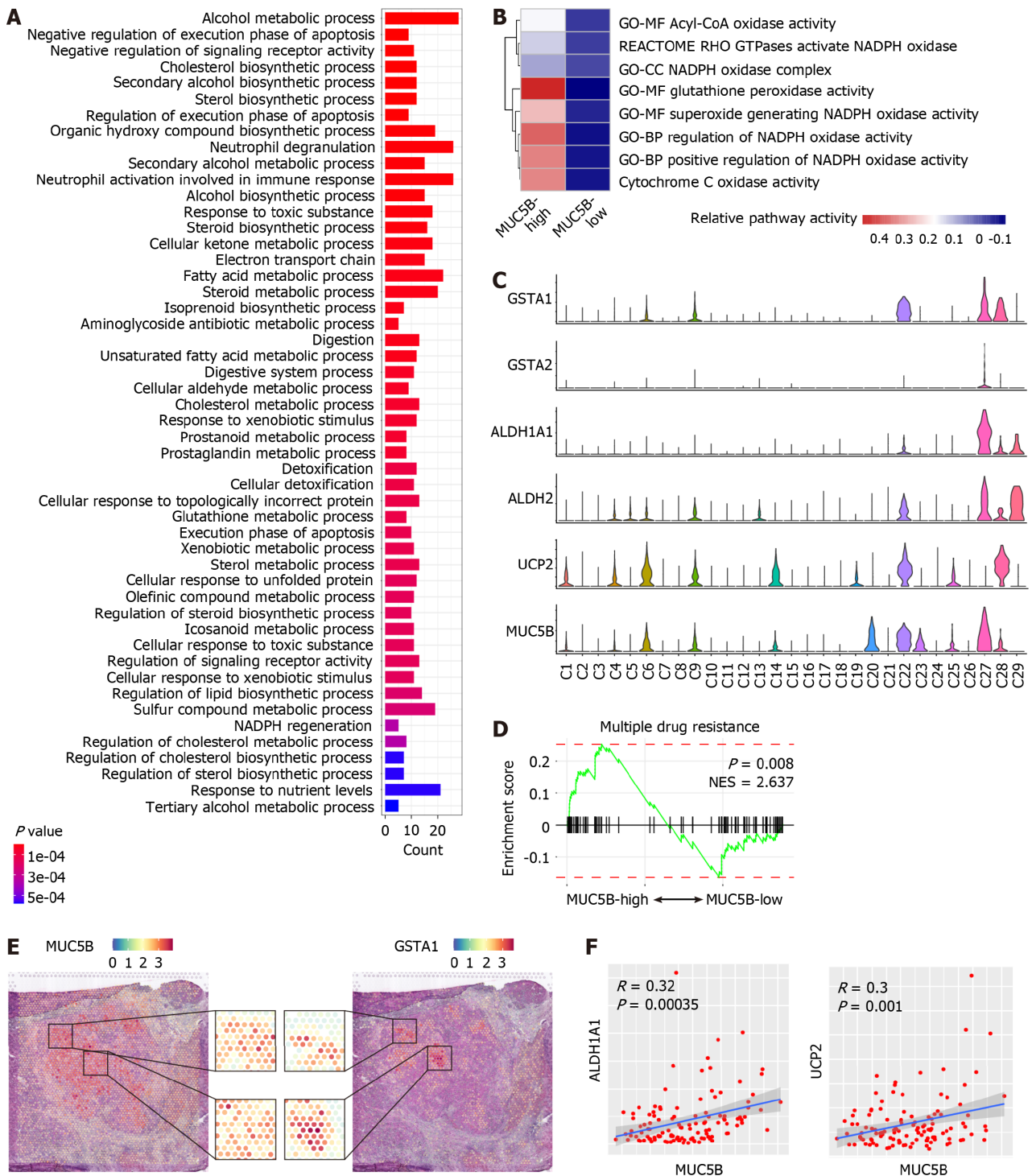


**Figure 4 Detoxification function of *MUC5B*-high tumor cells of cholangiocarcinoma.** A: Top 50 enriched signaling pathways of the differentially expressed genes in *MUC5B*-high cells; B: Heatmap showing the relative activities of oxidation-related metabolic signaling pathways in *MUC5B*-high vs *MUC5B*-low cells; C: Violin plots showing relative expression levels of *GSTA1*, *GSTA2*, *ALDH1A1*, *ALDH2*, *UCP2*, and *MUC5B* in cholangiocarcinoma (CCA) tumor sub-clusters; D: Gene set enrichment analysis plot showing the enrichment of genes from *MUC5B*-high (left) and *MUC5B*-low (right) cells in the drug resistance signaling pathway. The *P* value and normalized enrichment score are indicated on the plot; E: Distribution of *MUC5B* and *GSTA1* in the spatial transcriptomics (ST) slide. Zoomed in portions of the ST chip (middle) showing multiple areas of co-localization; F: Correlation analysis between the expression of *MUC5B* and *ALDH1A1* (left), *MUC5B* and *UCP2* (right) in CCA tumor samples from cohort 10.

### M2-polarization of macrophages induced by *MUC13*-high CCA cells

Although *MUC13* has been reported to play important roles in the progression of various tumors[38], the interaction between *MUC13*-high cells and the TME has not been fully elucidated. Considering the distinctive expression of *MUC13* in C23 and C29 (Figure 1C), we integrated C23 and C29 to generate *MUC13*-high CCA cells, while the remaining sub-clusters were categorized as *MUC13*-low cells. Interaction analyses between *MUC13*-high cells and TME components, namely *MUC13*-low cells, myeloid cells, endothelial cells, fibroblasts, and lymphocytes, revealed significant interactions

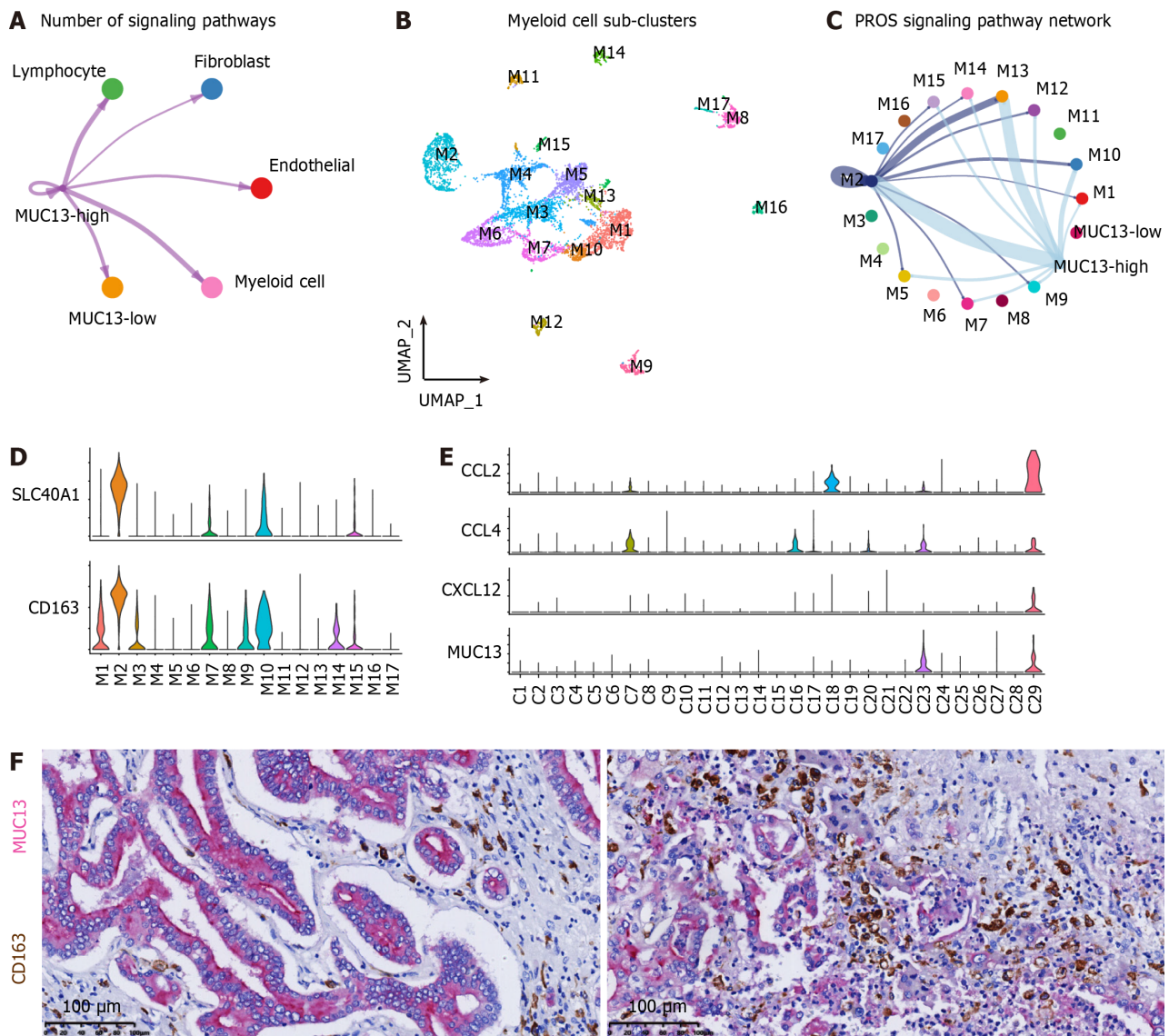


**Figure 5 Chemotaxis and M2-polarization of macrophage induced by *MUC13*-high tumor cells of cholangiocarcinoma.** A: Number of signaling pathways among *MUC13*-high, *MUC13*-low, myeloid cells, endothelial cells, fibroblasts, and lymphocytes; B: Uniform manifold approximation and projection plot showing the identification of 17 myeloid cell sub-clusters; C: PROS signaling pathway activity among the *MUC13*-high sub-cluster, *MUC13*-low sub-cluster, and myeloid cell sub-clusters; D: Violin plots showing relative expression levels of M2-polarized macrophage marker genes, including *SLC40A1* and *CD163*, in myeloid cell sub-clusters; E: Violin plots showing relative expression levels of *CCL2*, *CCL4*, and *CXCL12* in tumor cell sub-clusters; F: Immunohistochemistry double staining showing the adjacent distribution of *MUC13*-high cells (*MUC13*-positive, purple) and M2-polarized macrophages (*CD163*-positive, brown) in cholangiocarcinoma. Scale bar, 100  $\mu$ m.

between *MUC13*-high cells and myeloid cells (Figure 5A). To comprehensively evaluate the transcriptomic characteristics of the myeloid cell sub-populations interacting with *MUC13*-high cells, we isolated myeloid cell components and re-clustered them into 17 sub-populations (Figure 5B). In comparison with *MUC13*-low cells, *MUC13*-high cells exhibited a specific interaction with the M2 sub-cluster of myeloid cells in the PROS1-AXL signaling pathway (Figure 5C). The PROS signaling pathway, particularly the AXL receptor on the macrophage surface, has been shown to induce macrophage M2-polarization and tumor progression[39]. Therefore, the communication between *MUC13*-high cells and the M2 sub-cluster suggested that M2-polarization was induced by *MUC13*-high cells. Moreover, the M2 sub-cluster was characterized by high expression of *SLC40A1* (Supplementary Figure 7, red frame), which was reported to be a marker gene of macrophage M2-polarization[40]. Subsequently, we examined the expression of *SLC40A1* and another M2-polarization marker, *CD163*, in the myeloid sub-clusters of our data. The results indicated significantly elevated expression levels of both *SLC40A1* and *CD163* in the M2 sub-cluster (Figure 5D), confirming the M2-polarization of these cells. We next explored the mechanisms of these interactions, and identified uniquely expressed *CCL2*, *CCL4*, and *CXCL12* in *MUC13*-high clusters (Figure 5E). The chemokine activities of *CCL2* and *CCL4* in macrophage recruitment and *CXCL12* in macrophage M2-polarization suggest that *MUC13*-high cells recruit macrophages into the TME and induce M2 polarization[41]. Additionally, double staining IHC was used to confirm the histologically adjacent distribution between *MUC13*-high cells and M2-polarized macrophages in multiple CCA samples (Figure 5F). Taken together, these findings suggest that *MUC13*-high cells promote CCA progression by inducing M2-polarization of macrophages through the

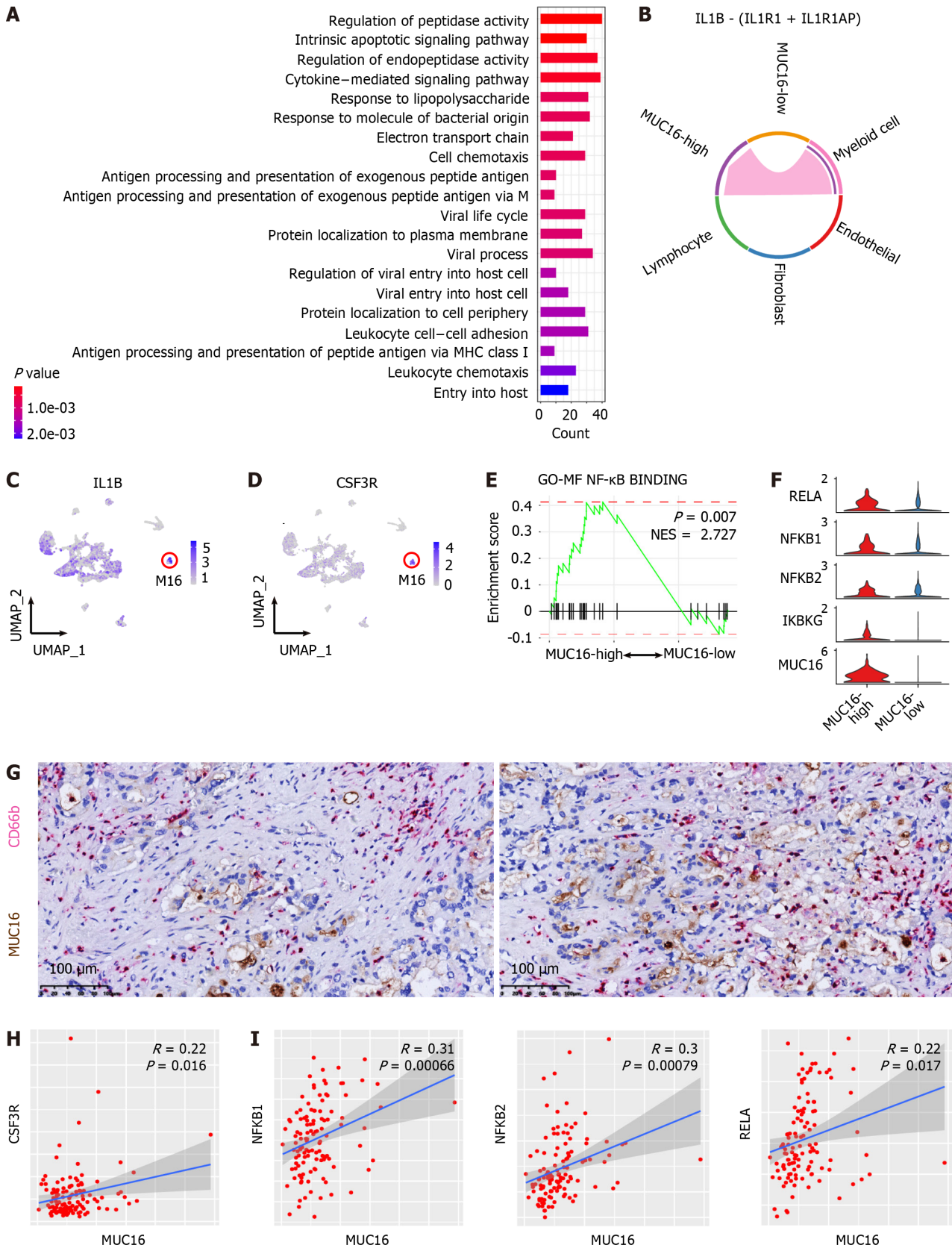


**Figure 6** Interaction with neutrophils and activated nuclear factor kappa-light-chain-enhancer of activated B cells signaling in *MUC16*-high tumor cells of cholangiocarcinoma. A: Top 20 enriched signaling pathways of the differentially expressed genes of *MUC16*-high cells; B: Interleukin-1 signaling pathway activity among *MUC16*-high cells, *MUC16*-low cells, and cells in tumor microenvironment; C and D: Feature-plots showing the expression level and distribution of *IL1B* and *CSF3R* in myeloid cell sub-clusters. Red circles showing the enrichment of *IL1B* and *CSF3R* in M16 sub-cluster; E: Gene set enrichment analysis plots showing the enrichment of genes from *MUC16*-high cells (left) and *MUC16*-low cells (right) in the nuclear factor kappa-light-chain-enhancer of activated B cells (NF-κB) signaling pathway. The *P* value and normalized enrichment score are indicated on the plot; F: Violin plots showing relative expression levels of key

regulatory genes (*RELA*, *NFKB1*, *NFKB2*, *IKBKKG*) of the NF- $\kappa$ B pathway in *MUC16*-high vs *MUC16*-low cells; G: Immunohistochemistry double staining showing the adjacent distribution of *MUC16*-high cells (*MUC16*-positive, brown) and neutrophils (CD66b-positive, purple) in cholangiocarcinoma (CCA). Scale bar, 100  $\mu$ m; H: Correlation analysis between the expression of *MUC16* and *CSF3R* in CCA tumor samples from cohort 10; I: Correlation analysis between the expression of *MUC16* and *NFKB1*, *NFKB2*, and *RELA* in CCA tumor samples from cohort 10.

PROS1-AXL signaling pathway.

### Activation of the NF- $\kappa$ B signaling pathway in *MUC16*-high CCA cells

*MUC16*, also known as CA125, serves as a widely used biomarker for ovarian cancer[42]. Nevertheless, the impact of *MUC16* on CCA progression and the underlying mechanisms remain elusive. Given the abundant and relatively unique expression of *MUC16* in the C20 cluster (Figure 1C), we designated the C20 cluster as *MUC16*-high cells, and the remaining sub-clusters were termed *MUC16*-low cells. To unravel the functions of *MUC16*, we first compared the transcriptomics of *MUC16*-high and *MUC16*-low cells. The enrichment of DEGs in *MUC16*-high cells revealed multiple pathways involved in immunoregulatory processes (Figure 6A). Therefore, we hypothesized interactions between *MUC16*-high cells and immune cells. Through an analysis of the interaction network of *MUC16*-high cells with cells in the TME, we identified unique interactions between myeloid cells and *MUC16*-high cells in the IL-1 signaling pathway, whereas *MUC16*-low cells did not show such interactions (Figure 6B). To further specify the sub-cluster of myeloid cells interacting with *MUC16*-high cells in the IL-1 signaling pathway, we examined the expression level of IL-1B in myeloid sub-clusters and found that the highest expression of IL-1B was in the M16 sub-cluster (Figure 6C). Intriguingly, M16 was characterized by high expression levels of *CXCL8*, *FCGR3B*, *NAMPT*, and *PTGS2* (Supplementary Figure 7, blue frame), indicating that M16 cells are a cluster of neutrophils. Consistently, *CSF3R*, a neutrophil marker[43], was found to be uniquely highly expressed in the M16 cluster (Figure 6D), supporting the interaction between *MUC16*-high cells and neutrophils through the IL1 signaling pathway. The activity of the IL-1 signaling pathway has been reported to be one of the most potent triggers for NF- $\kappa$ B signaling[44]. Therefore, we analyzed the activity of the NF- $\kappa$ B signaling in *MUC16*-high cells, and found significant enrichment of NF- $\kappa$ B signaling pathway genes in *MUC16*-high cells compared with *MUC16*-low cells (Figure 6E). To further confirm the activation of the NF- $\kappa$ B pathway in *MUC16*-high cells, we compared the expression levels of critical molecules in the NF- $\kappa$ B pathway, including *RELA*, *NFKB1*, *NFKB2*, and *IKBKKG*, and found that the expression levels of these molecules were greater in *MUC16*-high cells than in *MUC16*-low cells (Figure 6F). Double staining IHC was further employed to confirm the histological adjacent distribution between *MUC16*-high cells and neutrophils in multiple CCA samples (Figure 6G). Moreover, gene co-expression pattern detection in cohort 10 further validated the interaction between *MUC16*-high cells and neutrophils (Figure 6H) and the activation of NF- $\kappa$ B signaling in *MUC16*-high cells (Figure 6I). Taken together, these findings suggest that *MUC16*-high cells interact with neutrophils, and induce CCA progression through activation of the NF- $\kappa$ B signaling pathway.

### CCA prognosis prediction model based on mucin levels

Given the intricate yet pivotal roles of mucins in CCA progression, we aimed to establish a comprehensive prognostic assessment strategy for CCA using mucins systematically. The RNA levels of mucins in different CCA patients exhibited mosaic distribution features (Figure 7A). Therefore, we used the LASSO-Cox regression strategy to construct a CCA risk factor evaluation system based on the RNA levels of *MUC1*, *MUC4*, *MUC5AC*, *MUC5B*, *MUC13*, and *MUC16*. This resulted in the following formula: Risk factor =  $0.0297 \times \text{Expr}_{\text{MUC1}} + 0.0574 \times \text{Expr}_{\text{MUC4}} + 0.0501 \times \text{Expr}_{\text{MUC5AC}} + 0.0657 \times \text{Expr}_{\text{MUC5B}} + 0.0460 \times \text{Expr}_{\text{MUC13}} + 0.1217 \times \text{Expr}_{\text{MUC16}}$ . Survival analysis of high-risk CCA patients and low-risk CCA patients revealed a significant difference (Figure 7B), suggesting the efficacy of our CCA risk assessment system. The superior performance of the risk factor compared with that of the individual mucins was further confirmed by area under curve analysis (Supplementary Figure 8A). Notably, compared to low-risk CCA patients, high-risk CCA patients exhibited markedly greater cell proliferation (Figure 7C), tumor metastasis (Figure 7D), and antitumor drug resistance (Figure 7E and F), thereby providing additional confirmation of the mechanisms involving mucins as we established. Intriguingly, we then tested the applicability of the risk factor evaluation formula to other types of carcinoma, and found that this formula could effectively predict the prognosis of pancreatic carcinoma and pulmonary adenocarcinoma (Supplementary Figure 8B).

To assess the universality of the CCA risk evaluation system, we expanded the input of the formula from RNA levels to protein levels. The protein levels of mucins in CCA patients showed mosaic distribution features similar to those of the RNA levels (Supplementary Figure 8C). By applying mucin proteins to the risk factor formula, we stratified the CCA patients into two groups, namely the high-risk group and low-risk group. As a result, high-risk CCA patients showed significantly shorter survival than low-risk CCA patients (Figure 7G), consistent with the result obtained from mucin RNA. Additionally, CCA patients in the high-risk group showed a higher vascular invasion rate (Figure 7H), regional lymph node metastasis rate (Figure 7I), and TNM stage (Figure 7J), further verifying the worse prognosis of high-risk patients. Notably, we further confirmed the reliability of our risk factor evaluation system using data from cohort 10, which included 83 iCCA patients and 29 pCCA patients, and found that patients with a higher risk factor showed a significantly worse prognosis than those with a lower risk factor (Figure 7K). In conclusion, we construct a CCA risk assessment tool that can assess both the RNA and protein levels of mucins.

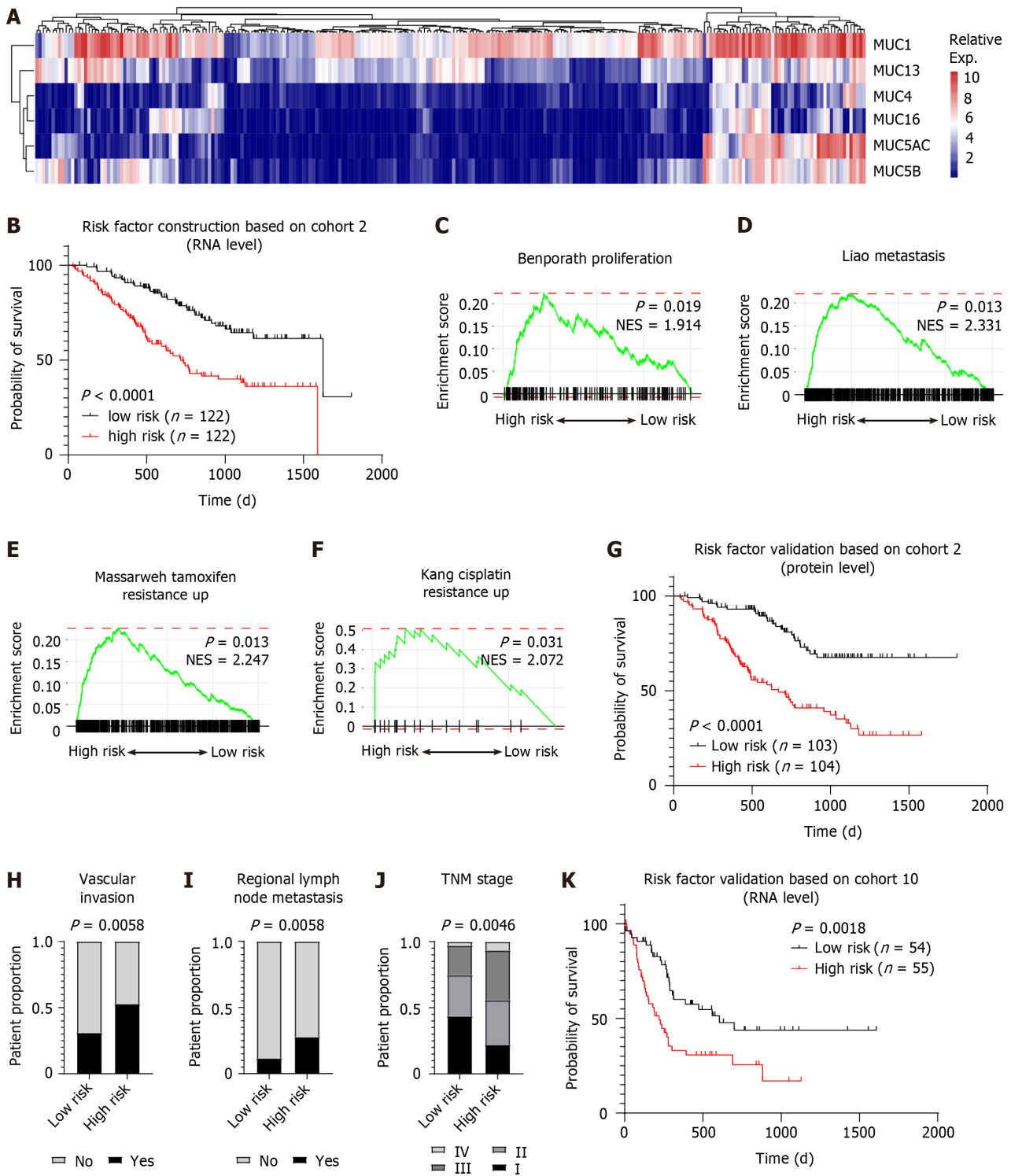


**Figure 7 Establishment of cholangiocarcinoma risk evaluation model based on mucin levels.** A: RNA levels of *MUC1*, *MUC13*, *MUC16*, *MUC4*, *MUC5AC* and *MUC5B* in cholangiocarcinoma (CCA) samples from cohort 2; B: Survival curve based on RNA levels of mucins showing the relationship between the risk factor and survival of CCA patients from cohort 2; C-F: Gene set enrichment analysis plots showing the enrichment of differentially expressed genes in high-risk patients in cell proliferation pathway, metastasis pathway, tamoxifen resistance pathway, and cisplatin resistance pathway. The *P* values and normalized enrichment score are indicated on the plots; G: Survival curve based on protein expression levels of mucins showing the relationship between the risk factor and survival of CCA patients from cohort 2; H-J: Correlation analyses of vascular invasion, regional lymph node metastasis, and tumor node metastasis stage with CCA risk factor; K: Survival curve based on RNA expression levels of mucins showing the relationship between the risk factor and survival of CCA patients from cohort 10.

## DISCUSSION

Mucins, a group of secretory proteins, play important roles in both physiological and pathological conditions. Elevated mucin levels have been observed in various tumor types, including CCA[10]. However, previous investigations into mucin functions in CCA have relied primarily on techniques such as IHC or enzyme-linked immunosorbent assay,

limiting the discovery of mucin functions to specific molecules. In contrast, in our study, we innovatively employed scRNA-seq for mucin investigation, which offers significant advantages in the following aspects: (1) Comprehensive analysis of the entire mucin family. In human, 21 mucins have been identified, with *MUC1*, *MUC4*, *MUC5AC*, and *MUC16* (CA125) being the most studied mucins in CCA. However, the functions of the remaining mucins in CCA are largely unknown. Our study considered the clinical significance and expression abundance of all mucins in CCA, leading to the identification of potential prognostic mucins, namely *MUC1*, *MUC4*, *MUC5AC*, *MUC5B*, *MUC13*, and *MUC16*; (2) Metabolic profiling of mucins. Metabolic reprogramming is a hallmark of cancer, and has drawn increased amounts of attention in CCA[45]. However, the metabolic states of mucin-positive cells in CCA have rarely been investigated. Our study is the first to report the metabolic characteristics of critical mucins in CCA. *FOSL1* and *HMGA1* were identified as critical transcription factors regulating active nucleotide metabolism in *MUC1*-high cells. Additionally, *GSTA1*, *GSTA2*, *ALDH1A1*, *ALDH2*, and *UCP2* were found to be overexpressed in *MUC5B*-high cells, regulating cellular oxidation processes to resist chemotherapies. These findings shed light on the mechanisms of CCA progression and treatment resistance in an unprecedented way; and (3) Interplay between mucin-positive cells and the TME. Despite numerous studies on *MUC1*-activated signaling pathways in tumor cells[10], the cellular interaction network between mucin-positive cells and TME components has seldom been illustrated. Using scRNA-seq data, we identified interactions between mucin-positive cells and myeloid cell sub-clusters. *MUC13*-high cells were found to induce macrophage infiltration into the TME, leading to subsequent M2-polarization through *PROS1*/*AXL* signaling. Additionally, *NF-κB* signaling pathway activation was observed in *MUC16*-high cells following interaction with neutrophils. These interactions elucidate the immunosuppressive status in CCA TME and offer potential targets for CCA immunotherapy. Although the number of patients used for functional mechanism investigations is limited, the CCA risk evaluation model based on mucin expression levels are applicable in large CCA cohorts, indicating the reliability of our conclusions.

Given its wide overexpression pattern and oncogenic characteristics, *MUC1* is anticipated to be a potential antitumor treatment target. However, the outcomes of clinical trials investigating *MUC1* have proven unsatisfactory[11,12]. Previous reports attributed this discrepancy to the scarcity of major histocompatibility complex class I epitopes within the *MUC1* protein, resulting in insufficient immune reactions[46]. Nevertheless, our data offer new possible explanations. Although *MUC1* is one of the most widely expressed mucins, there are numerous mucins, including *MUC4*, *MUC5AC*, *MUC5B*, *MUC13*, and *MUC16*, which share oncogenic and metabolic characteristics with *MUC1*. Therefore, targeting *MUC1* alone may be insufficient for effective tumor therapy. Our study developed a mucin-based CCA risk evaluation system that links risk factors to multiple CCA pathological indicators, such as tumor cell proliferation, metastasis, and resistance to antitumor drugs.

In fact, the risk factor formula, which includes *MUC1*, *MUC4*, *MUC5AC*, *MUC5B*, *MUC13*, and *MUC16*, implies the involvement and necessity of all six mucins in CCA development. Consequently, targeting all mucins together may yield more effective therapeutic outcomes than focusing solely on *MUC1*. Notably, although the functional mechanisms of mucin-positive cells may not be directly facilitated by mucins, mucin-directed immune therapy or chemotherapy still shows strong clinical application potential. Recently, *MUC1*-directed chimeric antigen receptor (CAR) T cell therapies have shown promising killing effects both *in-vitro* and *in-vivo*[47,48]. Our data reveal attractive targets for immunotherapy, suggesting that anti-*MUC4*, anti-*MUC5AC*, anti-*MUC5B*, anti-*MUC13* or anti-*MUC16* CAR T cells may also show promising treatment effects in the future.

Through a comprehensive approach involving both bioinformatic analysis strategies and experimental validation, our study successfully unveils the functional mechanisms of mucin-positive cells in CCA progression, through *MUC1*, *MUC4*, *MUC5AC*, *MUC5B*, *MUC13*, and *MUC16*. We subsequently construct a CCA risk factor evaluation system based on the expression levels of these six mucins. The risk factor evaluation model effectively predicts CCA patient prognosis, providing a novel patient stratification method. The results obtained in our study not only enrich the current understanding of mucins in CCA progression, but also identify new targets for precision treatments of CCA.

## CONCLUSION

In conclusion, we analyzed ten clinical CCA cohorts to investigate the functions of mucins on CCA progression and prognosis. The mucin family, includes *MUC1*, *MUC4*, *MUC5AC*, *MUC5B*, *MUC13*, and *MUC16*, regulates tumor metabolism, invasiveness, chemotherapy resistance, and cellular interaction with immune cells in microenvironments, comprehensively promoting CCA progression. We also construct a CCA risk evaluation model based on the expression levels of these mucins, applicable at both RNA and protein levels. Given the critical roles of these mucins on CCA development, our model serves as a promising tool for evaluating tumor malignancy and stratifying CCA patients.

## ARTICLE HIGHLIGHTS

### Research background

Cholangiocarcinoma (CCA) is the second most common type of liver cancer and exhibits a high mortality rate. Mucins are a family of protein that are elevated in various tumor types, including CCA. However, the comprehensive functional mechanisms and prognosis evaluation significance of mucins in CCA progression remain largely unknown.

**Research motivation**

*MUC1* has been identified as an oncogene that induce CCA progression through multiple signaling pathways. Nevertheless, how the mucin family regulate CCA is still elusive.

**Research objectives**

To investigate the functional mechanisms of mucins in CCA and to conduct a CCA risk evaluation model based on mucin expression levels.

**Research methods**

For the detection of mucin functions in CCA, single-cell RNA sequencing data from 14 CCA samples were employed, supported by comprehensive bioinformatic analyses. Validations were pursued through spatial transcriptomics and immunohistochemistry. The establishment of a CCA risk evaluation model based on mucin expression levels employed the least absolute shrinkage and selection operator regression algorithm. The risk evaluation model was constructed using RNA level of mucins, and subsequently validated by both RNA and protein levels of mucins, as well as multiple independent cohorts.

**Research results**

Elevated levels of *MUC1* and *MUC4* in CCA tumor cells were associated with activated nucleotide metabolic pathways and higher invasiveness. CCA tumor cells with heightened *MUC5AC* expression were found to induce tumor progression through the WNT signaling pathway. Robust cellular oxidation activities in *MUC5B*-high CCA tumor cells facilitated antitumoral treatment resistance. *MUC13*-high cells transformed macrophage into M2-polarization state through the PROS signaling and chemokines, including *CCL2*, *CCL4*, and *CXCR12*. Neutrophils induced the activation of nuclear factor kappa-light-chain-enhancer of activated B cells signaling in *MUC16*-high cells through the IL1B signaling, thereby promoting CCA development. Utilizing the expression levels of these mucins, a CCA prognosis evaluation model was developed and validated across multiple cohorts, which simultaneously exhibited predictive functions on the evaluation of CCA malignancy, metastasis potential, and chemotherapy sensitivity.

**Research conclusions**

Our study unveils the functional mechanisms by which mucins contribute to CCA progression, and offers a potential tool for CCA risk stratification.

**Research perspectives**

The discovery of mucin functions in CCA development and prognosis prediction indicate that mucins may be promising treatment targets for CCA.

---

**ACKNOWLEDGEMENTS**

We thank Guangze Zhang and Xin Zhang in Peking University Health Science Center for assistance in data analysis. We thank Prof. Jin Gu in Tsinghua University for ST data sharing.

---

**FOOTNOTES**

**Co-first authors:** Chun-Yuan Yang and Li-Mei Guo.

**Author contributions:** Yang CY and Guo LM provided study concept, design, and methodology of the paper; Yang CY, Guo LM, and Luo JY performed writing, review and revision of the paper; Yang CY, Li Y, Wang GX, Tang XW, Zhang QL, and Zhang LF performed acquisition, analysis and interpretation of data, and statistical analysis; Guo LM provided technical and material support. All authors read and approved the final paper. Yang CY and Guo LM contributed equally to this work and are designated as co-first authors for two main reasons. Firstly, our study was a result of collaborative efforts, with the design and conceptualization evolving through extensive discussions between Yang CY and Guo LM. Continuous communications ensured improvement of our manuscript at both pre-submission and post-submission stages. Secondly, the overall research team encompassed authors with diverse skills from various fields. Yang CY performed bioinformatic analyses, and Guo LM was responsible for clinical validation. The co-first authorship signature respected the collaboration of different expertise, ultimately enhancing the paper's quality and reliability. In summary, we believe that designating Yang CY and Guo LM as co-first authors of our manuscript as it accurately reflects our team's collaborative spirit and equal contributions.

**Institutional review board statement:** The study was reviewed and approved by the Science and Research Office of Peking University Third Hospital.

**Informed consent statement:** All study participants, or their legal guardian, provided informed written consent prior to study enrollment.

**Conflict-of-interest statement:** There are no conflicts of interest to report.

**Data sharing statement:** No additional data are available.

**STROBE statement:** The authors have read the STROBE Statement-checklist of items, and the manuscript was prepared and revised according to the STROBE Statement-checklist of items.

**Open-Access:** This article is an open-access article that was selected by an in-house editor and fully peer-reviewed by external reviewers. It is distributed in accordance with the Creative Commons Attribution NonCommercial (CC BY-NC 4.0) license, which permits others to distribute, remix, adapt, build upon this work non-commercially, and license their derivative works on different terms, provided the original work is properly cited and the use is non-commercial. See: <https://creativecommons.org/licenses/by-nc/4.0/>

**Country/Territory of origin:** China

**ORCID number:** Li-Mei Guo 0000-0002-4472-2705.

**S-Editor:** Qu XL

**L-Editor:** A

**P-Editor:** Zheng XM

## REFERENCES

- 1 Saha SK, Zhu AX, Fuchs CS, Brooks GA. Forty-Year Trends in Cholangiocarcinoma Incidence in the U.S.: Intrahepatic Disease on the Rise. *Oncologist* 2016; **21**: 594-599 [PMID: 27000463 DOI: 10.1634/theoncologist.2015-0446]
- 2 Khan SA, Taylor-Robinson SD, Toledano MB, Beck A, Elliott P, Thomas HC. Changing international trends in mortality rates for liver, biliary and pancreatic tumours. *J Hepatol* 2002; **37**: 806-813 [PMID: 12445422 DOI: 10.1016/s0168-8278(02)00297-0]
- 3 Rizvi S, Khan SA, Hallemeier CL, Kelley RK, Gores GJ. Cholangiocarcinoma - evolving concepts and therapeutic strategies. *Nat Rev Clin Oncol* 2018; **15**: 95-111 [PMID: 28994423 DOI: 10.1038/nrclinonc.2017.157]
- 4 Jarnagin WR, Fong Y, DeMatteo RP, Gonen M, Burke EC, Bodniewicz BS J, Youssef BA M, Klimstra D, Blumgart LH. Staging, resectability, and outcome in 225 patients with hilar cholangiocarcinoma. *Ann Surg* 2001; **234**: 507-17; discussion 517 [PMID: 11573044 DOI: 10.1097/00000658-200110000-00010]
- 5 Valle J, Wasan H, Palmer DH, Cunningham D, Anthoney A, Maraveyas A, Madhusudan S, Iveson T, Hughes S, Pereira SP, Roughton M, Bridgewater J; ABC-02 Trial Investigators. Cisplatin plus gemcitabine versus gemcitabine for biliary tract cancer. *N Engl J Med* 2010; **362**: 1273-1281 [PMID: 20375404 DOI: 10.1056/NEJMoa0908721]
- 6 Abou-Alfa GK, Sahai V, Hollebecque A, Vaccaro G, Melisi D, Al-Rajabi R, Paulson AS, Borad MJ, Gallinson D, Murphy AG, Oh DY, Dotan E, Catenacci DV, Van Cutsem E, Ji T, Lihou CF, Zhen H, Féliz L, Vogel A. Pemigatinib for previously treated, locally advanced or metastatic cholangiocarcinoma: a multicentre, open-label, phase 2 study. *Lancet Oncol* 2020; **21**: 671-684 [PMID: 32203698 DOI: 10.1016/S1470-2045(20)30109-1]
- 7 Kendall T, Verheij J, Gaudio E, Evert M, Guido M, Goeppert B, Carpino G. Anatomical, histomorphological and molecular classification of cholangiocarcinoma. *Liver Int* 2019; **39** Suppl 1: 7-18 [PMID: 30882996 DOI: 10.1111/liv.14093]
- 8 Leal J, Smyth HDC, Ghosh D. Physicochemical properties of mucus and their impact on transmucosal drug delivery. *Int J Pharm* 2017; **532**: 555-572 [PMID: 28917986 DOI: 10.1016/j.ijpharm.2017.09.018]
- 9 Dhanisha SS, Guruvayoorappan C, Drishya S, Abeesh P. Mucins: Structural diversity, biosynthesis, its role in pathogenesis and as possible therapeutic targets. *Crit Rev Oncol Hematol* 2018; **122**: 98-122 [PMID: 29458795 DOI: 10.1016/j.critrevonc.2017.12.006]
- 10 Kasprzak A, Adamek A. Mucins: the Old, the New and the Promising Factors in Hepatobiliary Carcinogenesis. *Int J Mol Sci* 2019; **20** [PMID: 30875782 DOI: 10.3390/ijms20061288]
- 11 Rossmann E, Österborg A, Löfvenberg E, Choudhury A, Forssmann U, von Heydebreck A, Schröder A, Mellstedt H. Mucin 1-specific active cancer immunotherapy with tecemotide (L-BLP25) in patients with multiple myeloma: an exploratory study. *Hum Vaccin Immunother* 2014; **10**: 3394-3408 [PMID: 25483677 DOI: 10.4161/hv.29918]
- 12 Butts C, Socinski MA, Mitchell PL, Thatcher N, Havel L, Krzakowski M, Nawrocki S, Ciuleanu TE, Bosquée L, Trigo JM, Spira A, Tremblay L, Nyman J, Ramlau R, Wickart-Johansson G, Ellis P, Gladkov O, Pereira JR, Eberhardt WE, Helwig C, Schröder A, Shepherd FA; START trial team. Tecemotide (L-BLP25) versus placebo after chemoradiotherapy for stage III non-small-cell lung cancer (START): a randomised, double-blind, phase 3 trial. *Lancet Oncol* 2014; **15**: 59-68 [PMID: 24331154 DOI: 10.1016/S1470-2045(13)70510-2]
- 13 Wang T, Xu C, Zhang Z, Wu H, Li X, Zhang Y, Deng N, Dang N, Tang G, Yang X, Shi B, Li Z, Li L, Ye K. Cellular heterogeneity and transcriptomic profiles during intrahepatic cholangiocarcinoma initiation and progression. *Hepatology* 2022; **76**: 1302-1317 [PMID: 35340039 DOI: 10.1002/hep.32483]
- 14 Song G, Shi Y, Meng L, Ma J, Huang S, Zhang J, Wu Y, Li J, Lin Y, Yang S, Rao D, Cheng Y, Lin J, Ji S, Liu Y, Jiang S, Wang X, Zhang S, Ke A, Cao Y, Ji Y, Zhou J, Fan J, Zhang X, Xi R, Gao Q. Single-cell transcriptomic analysis suggests two molecularly subtypes of intrahepatic cholangiocarcinoma. *Nat Commun* 2022; **13**: 1642 [PMID: 35347134 DOI: 10.1038/s41467-022-29164-0]
- 15 Affo S, Nair A, Brundu F, Ravichandra A, Bhattacharjee S, Matsuda M, Chin L, Filliol A, Wen W, Song X, Decker A, Worley J, Caviglia JM, Yu L, Yin D, Saito Y, Savage T, Wells RG, Mack M, Zender L, Arpaia N, Remotti HE, Rabadan R, Sims P, Leblond AL, Weber A, Riener MO, Stockwell BR, Gaublomme J, Llovet JM, Kalluri R, Michalopoulos GK, Seki E, Sia D, Chen X, Califano A, Schwabe RF. Promotion of cholangiocarcinoma growth by diverse cancer-associated fibroblast subpopulations. *Cancer Cell* 2021; **39**: 866-882.e11 [PMID: 33930309 DOI: 10.1016/j.ccell.2021.03.012]
- 16 Zhang M, Yang H, Wan L, Wang Z, Wang H, Ge C, Liu Y, Hao Y, Zhang D, Shi G, Gong Y, Ni Y, Wang C, Zhang Y, Xi J, Wang S, Shi L, Zhang L, Yue W, Pei X, Liu B, Yan X. Single-cell transcriptomic architecture and intercellular crosstalk of human intrahepatic cholangiocarcinoma. *J Hepatol* 2020; **73**: 1118-1130 [PMID: 32505533 DOI: 10.1016/j.jhep.2020.05.039]

- 17 **Aibar S**, González-Blas CB, Moerman T, Huynh-Thu VA, Imrichova H, Hulselmans G, Rambow F, Marine JC, Geurts P, Aerts J, van den Oord J, Atak ZK, Wouters J, Aerts S. SCENIC: single-cell regulatory network inference and clustering. *Nat Methods* 2017; **14**: 1083-1086 [PMID: 28991892 DOI: 10.1038/nmeth.4463]
- 18 **Gaude E**, Frezza C. Tissue-specific and convergent metabolic transformation of cancer correlates with metastatic potential and patient survival. *Nat Commun* 2016; **7**: 13041 [PMID: 27721378 DOI: 10.1038/ncomms13041]
- 19 **Wu R**, Guo W, Qiu X, Wang S, Sui C, Lian Q, Wu J, Shan Y, Yang Z, Yang S, Wu T, Wang K, Zhu Y, Liu C, Zhang Y, Zheng B, Li Z, Shen S, Zhao Y, Wang W, Bao J, Hu J, Wu X, Jiang X, Wang H, Gu J, Chen L. Comprehensive analysis of spatial architecture in primary liver cancer. *Sci Adv* 2021; **7**: eabg3750 [PMID: 34919432 DOI: 10.1126/sciadv.abg3750]
- 20 **Jusakul A**, Cutcutache I, Yong CH, Lim JQ, Huang MN, Padmanabhan N, Nellore V, Kongpetch S, Ng AWT, Ng LM, Choo SP, Myint SS, Thanan R, Nagarajan S, Lim WK, Ng CCY, Boot A, Liu M, Ong CK, Rajasegaran V, Lie S, Lim AST, Lim TH, Tan J, Loh JL, McPherson JR, Khuntikeo N, Bhudhisawasdi V, Yongvanit P, Wongkham S, Totoki Y, Nakamura H, Arai Y, Yamasaki S, Chow PK, Chung AYW, Ooi LLPJ, Lim KH, Dima S, Duda DG, Popescu I, Broet P, Hsieh SY, Yu MC, Scarpa A, Lai J, Luo DX, Carvalho AL, Vettore AL, Rhee H, Park YN, Alexandrov LB, Gordán R, Rozen SG, Shibata T, Pairojkul C, Teh BT, Tan P. Whole-Genome and Epigenomic Landscapes of Etiologically Distinct Subtypes of Cholangiocarcinoma. *Cancer Discov* 2017; **7**: 1116-1135 [PMID: 28667006 DOI: 10.1158/2159-8290.CD-17-0368]
- 21 **Jin S**, Guerrero-Juarez CF, Zhang L, Chang I, Ramos R, Kuan CH, Myung P, Plikus MV, Nie Q. Inference and analysis of cell-cell communication using CellChat. *Nat Commun* 2021; **12**: 1088 [PMID: 33597522 DOI: 10.1038/s41467-021-21246-9]
- 22 **Abe T**, Amano H, Shimamoto F, Hattori M, Kuroda S, Kobayashi T, Tashiro H, Ohdan H. Prognostic evaluation of mucin-5AC expression in intrahepatic cholangiocarcinoma, mass-forming type, following hepatectomy. *Eur J Surg Oncol* 2015; **41**: 1515-1521 [PMID: 26210654 DOI: 10.1016/j.ejso.2015.07.006]
- 23 **Pabalan N**, Sukcharoensin S, Butthongkomvong K, Jarjanazi H, Thitapakorn V. Expression and Serum Levels of Mucin 5AC (MUC5AC) as a Biomarker for Cholangiocarcinoma: a Meta-analysis. *J Gastrointest Cancer* 2019; **50**: 54-61 [PMID: 29139058 DOI: 10.1007/s12029-017-0032-9]
- 24 **Dong L**, Lu D, Chen R, Lin Y, Zhu H, Zhang Z, Cai S, Cui P, Song G, Rao D, Yi X, Wu Y, Song N, Liu F, Zou Y, Zhang S, Zhang X, Wang X, Qiu S, Zhou J, Wang S, Shi Y, Figeys D, Ding L, Wang P, Zhang B, Rodriguez H, Gao Q, Gao D, Zhou H, Fan J. Proteogenomic characterization identifies clinically relevant subgroups of intrahepatic cholangiocarcinoma. *Cancer Cell* 2022; **40**: 70-87.e15 [PMID: 34971568 DOI: 10.1016/j.ccell.2021.12.006]
- 25 **Andersen JB**, Spee B, Blechacz BR, Avital I, Komuta M, Barbour A, Conner EA, Gillen MC, Roskams T, Roberts LR, Factor VM, Thorgeirsson SS. Genomic and genetic characterization of cholangiocarcinoma identifies therapeutic targets for tyrosine kinase inhibitors. *Gastroenterology* 2012; **142**: 1021-1031.e15 [PMID: 22178589 DOI: 10.1053/j.gastro.2011.12.005]
- 26 **Ahn KS**, O'Brien D, Kang YN, Mounajjed T, Kim YH, Kim TS, Kocher JA, Allotey LK, Borad MJ, Roberts LR, Kang KJ. Prognostic subclass of intrahepatic cholangiocarcinoma by integrative molecular-clinical analysis and potential targeted approach. *Hepatol Int* 2019; **13**: 490-500 [PMID: 31214875 DOI: 10.1007/s12072-019-09954-3]
- 27 **Ma L**, Hernandez MO, Zhao Y, Mehta M, Tran B, Kelly M, Rae Z, Hernandez JM, Davis JL, Martin SP, Kleiner DE, Hewitt SM, Ylaja K, Wood BJ, Greten TF, Wang XW. Tumor Cell Biodiversity Drives Microenvironmental Reprogramming in Liver Cancer. *Cancer Cell* 2019; **36**: 418-430.e6 [PMID: 31588021 DOI: 10.1016/j.ccell.2019.08.007]
- 28 **Maurus K**, Hufnagel A, Geiger F, Graf S, Berking C, Heinemann A, Paschen A, Kneitz S, Stigloher C, Geissinger E, Otto C, Bosserhoff A, Schartl M, Meierjohann S. The AP-1 transcription factor FOSL1 causes melanocyte reprogramming and transformation. *Oncogene* 2017; **36**: 5110-5121 [PMID: 28481878 DOI: 10.1038/nc.2017.135]
- 29 **Xu M**, Sharma P, Pan S, Malik S, Roeder RG, Martinez E. Core promoter-selective function of HMGAl and Mediator in Initiator-dependent transcription. *Genes Dev* 2011; **25**: 2513-2524 [PMID: 22156211 DOI: 10.1101/gad.177360.111]
- 30 **Adair JE**, Maloney SC, Dement GA, Wertzler KJ, Smerdon MJ, Reeves R. High-mobility group A1 proteins inhibit expression of nucleotide excision repair factor xeroderma pigmentosum group A. *Cancer Res* 2007; **67**: 6044-6052 [PMID: 17616660 DOI: 10.1158/0008-5472.Can-06-1689]
- 31 **Zhang M**, Hoyle RG, Ma Z, Sun B, Cai W, Cai H, Xie N, Zhang Y, Hou J, Liu X, Chen D, Kellogg GE, Harada H, Sun Y, Wang C, Li J. FOSL1 promotes metastasis of head and neck squamous cell carcinoma through super-enhancer-driven transcription program. *Mol Ther* 2021; **29**: 2583-2600 [PMID: 33794365 DOI: 10.1016/j.ymthe.2021.03.024]
- 32 **Zhan T**, Rindtorff N, Boutros M. Wnt signaling in cancer. *Oncogene* 2017; **36**: 1461-1473 [PMID: 27617575 DOI: 10.1038/nc.2016.304]
- 33 **Han B**, Zhou B, Qu Y, Gao B, Xu Y, Chung S, Tanaka H, Yang W, Giuliano AE, Cui X. FOXC1-induced non-canonical WNT5A-MMP7 signaling regulates invasiveness in triple-negative breast cancer. *Oncogene* 2018; **37**: 1399-1408 [PMID: 29249801 DOI: 10.1038/s41388-017-0021-2]
- 34 **Xu M**, Wang Y, Duan W, Xia S, Wei S, Liu W, Wang Q. Proteomic Reveals Reasons for Acquired Drug Resistance in Lung Cancer Derived Brain Metastasis Based on a Newly Established Multi-Organ Microfluidic Chip Model. *Front Bioeng Biotechnol* 2020; **8**: 612091 [PMID: 33415100 DOI: 10.3389/fbioe.2020.612091]
- 35 **Liu H**, Yang Z, Zang L, Wang G, Zhou S, Jin G, Pan X. Downregulation of Glutathione S-transferase A1 suppressed tumor growth and induced cell apoptosis in A549 cell line. *Oncol Lett* 2018; **16**: 467-474 [PMID: 29928434 DOI: 10.3892/ol.2018.8608]
- 36 **Kleih M**, Böppele K, Dong M, Gaißler A, Heine S, Olayioye MA, Aulitzky WE, Essmann F. Direct impact of cisplatin on mitochondria induces ROS production that dictates cell fate of ovarian cancer cells. *Cell Death Dis* 2019; **10**: 851 [PMID: 31699970 DOI: 10.1038/s41419-019-2081-4]
- 37 **Cubillos-Ruiz JR**, Bettigole SE, Glimcher LH. Tumorigenic and Immunosuppressive Effects of Endoplasmic Reticulum Stress in Cancer. *Cell* 2017; **168**: 692-706 [PMID: 28187289 DOI: 10.1016/j.ccell.2016.12.004]
- 38 **Maher DM**, Gupta BK, Nagata S, Jaggi M, Chauhan SC. Mucin 13: structure, function, and potential roles in cancer pathogenesis. *Mol Cancer Res* 2011; **9**: 531-537 [PMID: 21450906 DOI: 10.1158/1541-7786.MCR-10-0443]
- 39 **Myers KV**, Amend SR, Pienta KJ. Targeting Tyro3, Axl and MerTK (TAM receptors): implications for macrophages in the tumor microenvironment. *Mol Cancer* 2019; **18**: 94 [PMID: 31088471 DOI: 10.1186/s12943-019-1022-2]
- 40 **Zhang Q**, He Y, Luo N, Patel SJ, Han Y, Gao R, Modak M, Carotta S, Haslinger C, Kind D, Peet GW, Zhong G, Lu S, Zhu W, Mao Y, Xiao M, Bergmann M, Hu X, Kerkar SP, Vogt AB, Pflanz S, Liu K, Peng J, Ren X, Zhang Z. Landscape and Dynamics of Single Immune Cells in Hepatocellular Carcinoma. *Cell* 2019; **179**: 829-845.e20 [PMID: 31675496 DOI: 10.1016/j.ccell.2019.10.003]
- 41 **Ruytinx P**, Proost P, Van Damme J, Struyf S. Chemokine-Induced Macrophage Polarization in Inflammatory Conditions. *Front Immunol* 2018; **9**: 1930 [PMID: 30245686 DOI: 10.3389/fimmu.2018.01930]

- 42 **Dochez V**, Caillon H, Vaucel E, Dimet J, Winer N, Ducarme G. Biomarkers and algorithms for diagnosis of ovarian cancer: CA125, HE4, RMI and ROMA, a review. *J Ovarian Res* 2019; **12**: 28 [PMID: 30917847 DOI: 10.1186/s13048-019-0503-7]
- 43 **Xue R**, Zhang Q, Cao Q, Kong R, Xiang X, Liu H, Feng M, Wang F, Cheng J, Li Z, Zhan Q, Deng M, Zhu J, Zhang Z, Zhang N. Liver tumour immune microenvironment subtypes and neutrophil heterogeneity. *Nature* 2022; **612**: 141-147 [PMID: 36352227 DOI: 10.1038/s41586-022-05400-x]
- 44 **Diep S**, Maddukuri M, Yamauchi S, Geshow G, Delk NA. Interleukin-1 and Nuclear Factor Kappa B Signaling Promote Breast Cancer Progression and Treatment Resistance. *Cells* 2022; **11** [PMID: 35626710 DOI: 10.3390/cells11101673]
- 45 **Raggi C**, Taddei ML, Rae C, Braconi C, Marra F. Metabolic reprogramming in cholangiocarcinoma. *J Hepatol* 2022; **77**: 849-864 [PMID: 35594992 DOI: 10.1016/j.jhep.2022.04.038]
- 46 **Taylor-Papadimitriou J**, Burchell JM, Graham R, Beatson R. Latest developments in MUC1 immunotherapy. *Biochem Soc Trans* 2018; **46**: 659-668 [PMID: 29784646 DOI: 10.1042/BST20170400]
- 47 **Supimon K**, Sangsuwannukul T, Sujjitoon J, Phanthaphol N, Chieochansin T, Pongvarin N, Wongkham S, Junking M, Yenichitsomanus PT. Anti-mucin 1 chimeric antigen receptor T cells for adoptive T cell therapy of cholangiocarcinoma. *Sci Rep* 2021; **11**: 6276 [PMID: 33737613 DOI: 10.1038/s41598-021-85747-9]
- 48 **Mao L**, Su S, Li J, Yu S, Gong Y, Chen C, Hu Z, Huang X. Development of Engineered CAR T Cells Targeting Tumor-Associated Glycoforms of MUC1 for the Treatment of Intrahepatic Cholangiocarcinoma. *J Immunother* 2023; **46**: 89-95 [PMID: 36883998 DOI: 10.1097/CJI.0000000000000460]



Published by **Baishideng Publishing Group Inc**  
7041 Koll Center Parkway, Suite 160, Pleasanton, CA 94566, USA  
**Telephone:** +1-925-3991568  
**E-mail:** [office@baishideng.com](mailto:office@baishideng.com)  
**Help Desk:** <https://www.f6publishing.com/helpdesk>  
<https://www.wjgnet.com>

